AN ABSTRACT OF THE THESIS OF

Shweta Paralikar for the degree of Master of Science in Wood Science and Chemical Engineering presented on June 9, 2006.

Title: Poly(vinyl alcohol) / Cellulose Nanocomposite Barrier Films.

Abstract approved:

John Simonsen Willie E. "Skip" Rochefort

There is a continual interest in developing robust, flexible, durable, lightweight, waterborne polymer barrier coatings which are increasingly resistant towards both chemical warfare agents as well as an ever growing number of toxic industrial chemicals. In this study, barrier films were prepared with poly(vinyl alcohol) (PVOH) and varying amounts of cellulose nanocrystals (CNXLs) as filler. Poly(acrylic acid) (PAA) was used as a crosslinking agent to provide water resistance to PVOH. The films were heat treated at various temperatures (125, 150, 170, 185 °C) in order to determine the optimum crosslinking density. Heat treatment at 170 °C for 45 minutes resulted in films with improved water resistance without polymer degradation. Infrared spectroscopy (FTIR) indicated ester bond formation with heat treatment. Mechanical tests showed that films with 10%CNXLs/ 10%PAA/ 80%PVOH had the highest tensile strength, tensile modulus

and toughness of all the films studied. Polarized optical microscopy and atomic force microscopy showed agglomeration of CNXLs at filler loadings of 15% CNXLs. A thermogravimetric analysis (DTGA) showed highly synergistic effects with 10%CNXLs/ 10%PAA/ 80%PVOH and supported the tensile test results.

The purpose of these barrier films is to prevent the diffusion of chemical warfare agents while allowing moisture to pass through to allow breathability. Water vapor transmission indicated that all the films allowed moisture to pass. However, moisture diffusion was reduced by the presence of both CNXLs and PAA compared to pure PVOH. The crystalline nature of CNXLs causes the diffusing molecules to undergo a tortuous path, while the crosslinking forms a network structure which reduces diffusion. A standard time lag diffusion test utilizing permeation cups was used to study the chemical barrier properties. The film containing 10%CNXL/ 10%PAA/ 80%PVOH showed an improvement of 90% compared to 100% PVOH film. Surface modification of CNXLs was successful and well dispersed carboxylated CNXLs were obtained. Carboxylated cellulose nanocrystals (C.CNXLs) showed less agglomeration, improved interaction, slightly reduced flux and slightly increased time lags compared to CNXLs.

Poly(vinyl alcohol) / Cellulose Nanocomposite Barrier Films

by
Shweta Paralikar

A THESIS

submitted to

Oregon State University

in partial fulfillment of
the requirements for the
degree of

Master of Science

Presented June 9, 2006
Commencement June 2007

Master of Science thesis of Shweta Paralikar presented on June 9, 2006.

APPROVED:

Co-Major Professor, representing Wood Science

Co-Major Professor, representing Chemical Engineering

Head of the Department of Wood Science

Head of the Department of Chemical Engineering

Dean of the Graduate School

I understand that my thesis will become part of the permanent collection of Oregon State University libraries. My signature below authorizes release of my thesis to any reader upon request.

Shweta Paralikar, Author

ACKNOWLEDGEMENTS

I sincerely thank my advisor, Dr. John Simonsen, for giving me the opportunity to work on this project, and for his guidance which was essential to the completion of my masters thesis.

I am grateful to Dr. Skip Rochefort, Dr. Joe Karchesy, Dr. Christine Kelly and Dr. David Cann for agreeing to serve on my committee and for taking time to review my thesis. Particular thanks goes to Dr. Skip Rochefort letting me use his DSC and TGA and for always showing concern about my career.

I thank the professors from Wood Science and Chemical Engineering departments for putting in great efforts in designing the courses as well as making them interesting.

I thank Mr. Michael Nesson for his help in sample preparation for AFM and SEM. I also thank Mr. Al Soeldner for obtaining the SEM pictures.

I enjoyed being part of the various functions and festivals celebrated by the Indian community in Corvallis. They offered a great way of destressing myself.

In giving appreciation, I must acknowledge my parents for their unwavering love and support all through my life. I thank my brother and my sister in law for being such great friends. I extend my appreciation to my in-laws and all relatives who have provided me a encouraging atmosphere and have been patient in waiting for me to finish this task. Above all, I thank my loving husband, Sanjit, without whom this would not have been possible.

CONTRIBUTION OF AUTHORS

The idea for the project was provided by Dr. John Lombardi of Ventana research coporation in Tucson, Arizona. He gave valuable suggestions in designing CVTR experiments. Dr. John Simonsen helped with planning of the overall scheme of experiments. He also helped with writing of Chapter 2 and Chapter 3.

TABLE OF CONTENTS

TABLE OF CONTENTS (continued)

LIST OF FIGURES

LIST OF FIGURES (continued)

LIST OF APPENDICES

LIST OF APPENDIX TABLES

Introduction

Introduction

Nanotechnology, though in a nascent stage, is currently one of the most promising arenas of technological development and is projected to have explosive growth in coming years.[1] The most accepted definition, as listed on the NASA website is 'The creation of functional materials, devices and systems through control of matter on the nanometer length scale (1-100 nanometers), and exploitation of novel phenomena and properties (physical, chemical, biological) at that length scale.'[2] Simply put 'nanotechnology' is the application of science which leads to technological developments at the nanometer scale.

The incorporation of nanoscale materials (at least one dimension is < 100 nm) into polymer matrices has created a broad range of novel applications with conventional polymers. Within the composite industry the idea of adding fillers into polymers is not a new one.[3] Many polymer composites have been commercialized for a very long time. However, nanoscale materials can offer further improvements in mechanical, thermal, electrical and barrier properties compared to conventional composites. These effects are largely due to their high interfacial area, their aspect ratio, their extent of dispersion and percolation, which occurs when the filler particles are present in quantities above the threshold where they start physically interacting and form a continous network.[4] Over and above these enormous implications on properties, some nanomaterials reduce the density of the overall composite as preferred properties are realized at far less filler content.[5] This is appealing, as novel materials with desired properties can then also be lightweight and durable.

Nanocrystalline cellulose is the filler material of interest in our laboratory. Cellulose is a natural biopolymer which is renewable, biodegradable and abundantly available. It can be obtained from various sources like wood, some bacteria, some algae, tunicates (a sea animal), grasses, etc. Compared to other nanomaterials it is low in cost and density (Table B.1) with a high aspect ratio (length/diameter) between 30 – 150 depending on the source from which it is obtained.[6, 7] It has higher strength than steel and higher stiffness than aluminum. It has high elastic modulus and strength reported to be 145 GPa[8] and 7500 MPa respectively.[9]

Cellulose is a homopolysaccharide consisting of β-D-glucopyranose units linked by glucoside bond at their C1 and C4 hydroxyl groups. (Figure 1.1)

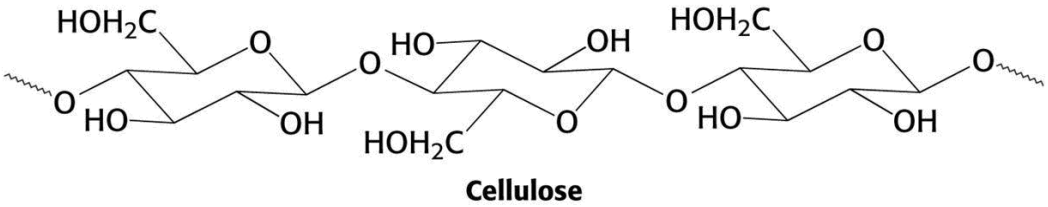

Figure 1.1. Structure of cellulose.

In nature cellulose occurs as aggregates which form microfibrils, within which highly ordered crystalline regions alternate with less ordered amorphous regions.[10] Cellulose nanocrystals are the crystalline portion of cellulose. Acid hydrolysis is an accepted method of producing cellulose nanocrystals, which was reported by Ranby 40 years ago.[11] Acid hydrolysis breaks down the microfibrils into elementary single crystallites.(Figure 1.2)

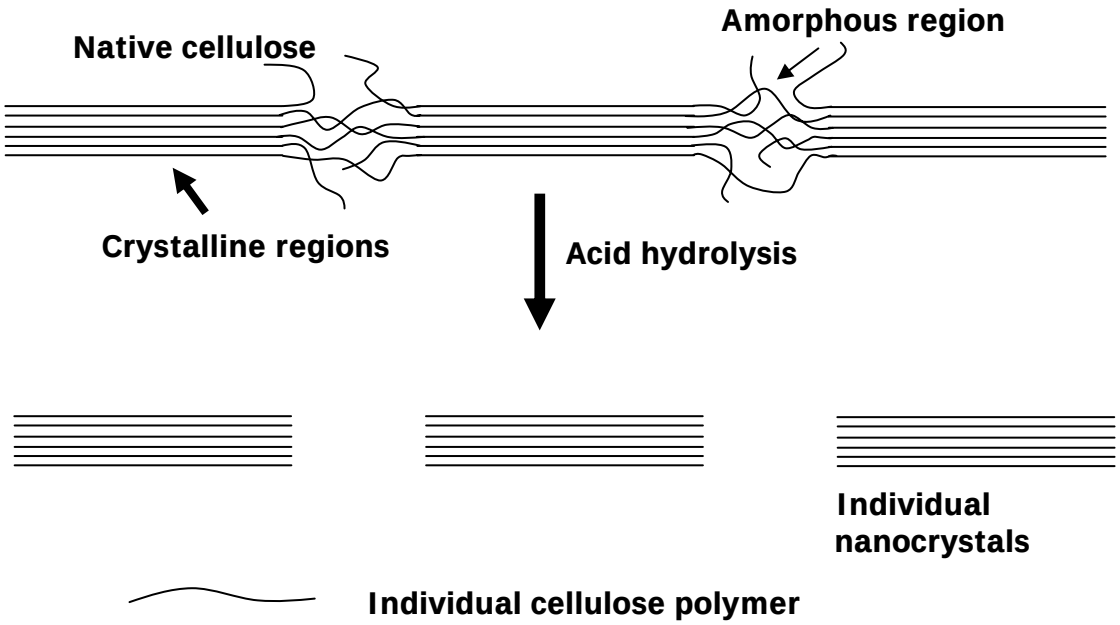

Figure 1.2. Acid hydrolysis of cellulose to form cellulose nanocrystals.

The average dimensions of crystallites produced from cotton are about 4 nm in diameter and 300 nm in length.[6] The acid hydrolysis of cellulose fibers is a heterogeneous acid diffusion process wherein acid penetrates the less ordered amorphous regions and causes the scission of glycosidic bonds. The penetration and the glycosidic bond breakage depend on the hydrolysis conditions, mainly the acid type, hydrolysis temperature, and acid concentration.[12] The reaction proceeds until all the accessible glycosidic bonds are hydrolyzed and later slows down significantly as the acid attacks the reducing end and the surface of the residual crystalline regions. Hydrolysis conditions should be mild enough to avoid complete hydrolysis of cellulose to glucose or even carbonization. Acid hydrolysis is done using either hydrochloric acid or sulfuric acid. Dong et.al has showed that a hydrolysis

temperature of 45 ^{o}C and hydrolysis time of 60 min are optimum conditions to achieve complete hydrolysis of the amorphous regions and a particle length in the order of 200 nm.[13] Although, the cellulose nanocrystals thus obtained have high specific strength and stiffness they are brittle if used by themselves. They can provide excellent properties when they are incorporated within a polymeric matrix and act as a reinforcing filler. Well dispersed cellulose nanocrystals can also act as a barrier to diffusing vapor as vapors cannot pass through the crystal structure.[14]

There are certain limitations with using cellulose nanocrystals, the most prominent being fiber matrix adhesion and cellulose agglomeration. Nanocrystalline cellulose is a hydrophilic polymer and hence when it is used with a hydrophobic polymer there is an inherent problem with fiber matrix interaction. This limitation is overcome with the addition of compatibilizers (coupling agents) which bridge the gap between filler and matrix and thereby improve fiber dispersion and wettability. Interface adhesion is usually not a problem when cellulose is blended with a hydrophilic polymer matrix. At the same time cellulose agglomeration can often be avoided by mixing the polymer and cellulose in an aqueous medium, followed by reactive drying or solvent evaporation.

In the study reported herein, we are using a system of poly(vinyl alcohol)/ poly(acrylic acid) and cellulose nanocrystals. Poly(vinyl alcohol) (PVOH) is a versatile polymer with varied commercial applications.[15] PVOH is prepared from hydrolyzing poly(vinyl acetate). There are several grades of this polymer and its basic properties greatly depend on its degree of polymerization and degree of hydrolysis.

Partially hydrolysed grades contain residual acetate groups which are esstentially hydrophobic, and weaken the intra and intermolecular hydrogen bonding of adjoining hydroxyl groups. The presence of these acetate groups in an adequate number reduces the degree of crystallinity within the polymer. The grade used for this study is 99+ % hydrolysed, which mean 99+ % of hydroxyl groups are available while there is < 1% of acetate groups are present (Figure 1.3).

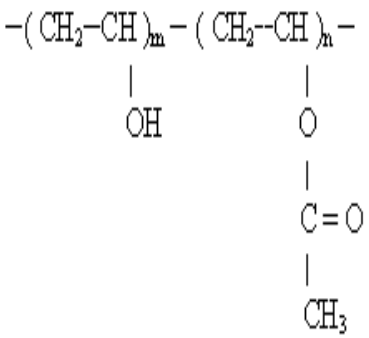

Figure 1.3. Structure of 99+ % hydrolyzed poly(vinyl alcohol). m= 99+ % hydroxyl groups, n = < 1% acetate groups.

PVOH films have poor stability in water unless crosslinked.[16] Some applications require PVOH to be water insoluble or resistant to swelling caused by water, for such cases PVOH mild crosslinking can be accomplised by heat treatment.[15] Crosslinking can also be achieved by adding crosslinking agents. The third component in this study is poly(acrylic acid) (PAA), which is a successful crosslinking agent for PVOH.[17] The addition of PAA along with heat treatment results in the formation of covalent ester linkages between PVOH and PAA (Figure 1.4)[18]

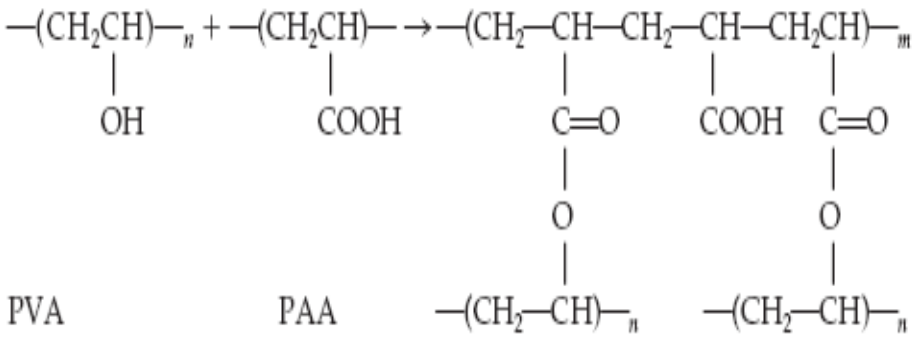

Figure 1.4. Expected crosslinking structure of heat treated poly(vinyl alcohol) (popularly represented as PVA/PVOH) and poly(acrylic acid) (PAA)[18]

However, CNXL structure also contains hydroxyl groups and they may also form ester linkages with PAA. Thus, it is possible for all the three components of the system studied herein to be chemically linked.(Figure 1.5)

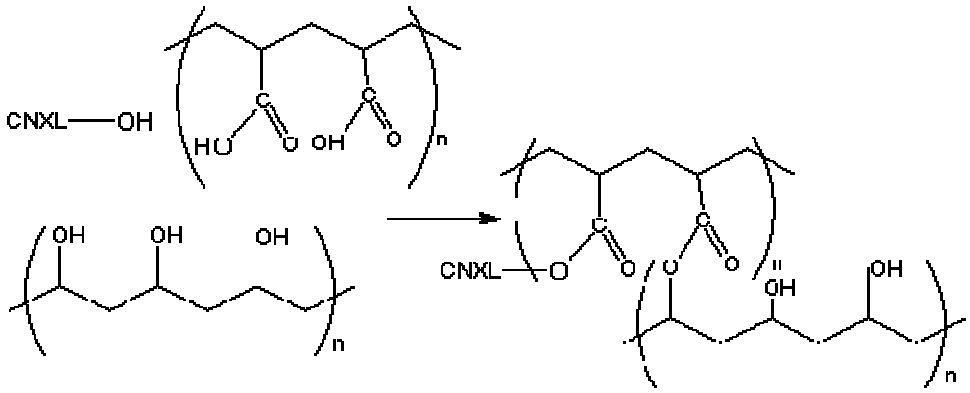

Figure 1.5. Proposed crosslinking scheme of PVOH/ PAA/ CNXLs system.

The objective of this study is to understand the chemical principles underlying the barrier film behavior and to find a combination of all the three components which will act as a effective barrier film. The purpose of these barrier films is to have the ability to prevent diffusion of harmful chemicals and be chemically inert, mechanically strong and tough, flexible and water resistant. Research in this area is

evolving rapidly to enhance the barrier properties and overcome certain limitations like durability, robustness, flexibility, cost, weight, and packing volume amongst several others.[19] One goal of this study is to provide tough, flexible films which will retard or reduce the diffusion of chemical warfare agents as well as toxic industrial chemicals through them. Chapter 2 reports mechanical properties, thermal properties and water solubility. Significant improvements in performance were observed. Dispersion of CNXLs was observed with various microscopic techniques. Chapter 3 reports experimental results for the ultimate application of the composite as a barrier film. The water vapor and chemical vapor transmission rate were tested. These results suggested 10%CNXL/ 10%PAA/ 80% PVOH film significantly improved performance. CNXLs were also carboxylated in order to observe any improvement in performance that resulted. While minor improvements in barrier performace were observed, a significant improvement in the dispersion of the carboxylated CNXLs was observed in comparison to non-carboxylated CNXLs. This resulted in improved properties in certain samples.

Bibliography

1. Havancsak K., Nanotechnology at present and its promises in the future. *Material Science Forum* **2003,** 414-415, 85-94.
2. NASA., http://www.ipt.arc.nasa.gov/nanotechnology.html.
3. Bor J., Advanced polymer composites: Principles and applications; ASM International: Materials Park, **1994**, 1-279.
4. Brechet Y; Cavaille J; Chabert E; Chazeau L; Dendievel R; Flandin L; Gauthier C., Polymer based nanocomposites: Effect of filler-filler and filler-matrix interactions. *Advanced engineering materials* **2001,** 3, 571.207.
5. Giannelis E., Polymer-Layered silicate nanocomposites: Synthesis, properties and applications. *Applied organometallic chemistry* **1998,** 12, 675-680.
6. Favier V; Chanzy H; Cavaille J., Polymer Nanocomposites reinforced by cellulose whiskers. *Macromolecules* **1995,** 28, (18), 6365-6367.
7. Dufresne A; Kellerhals M; Witholt B., Transcrystallinzation in Mcl-PHAs/Cellulose whiskers composites. *Macromolecules* **1999,** 32, 7396.
8. Eichhorn S; Baillie C; Zafereiropoulos N; Mwaikambo L; Ansell M; Dufresne A; Entwistle K; Herrera-Franco P; Escamilla G; Groom L; Hughes M; Hill C; Rials T., Review- Current international research into cellulosic fibres and composites. *Journal of Material Science* **2001,** 36, 2107.
9. Marks R., Cell wall mechanics of tracheids. *Cell wall mechanics of tracheids*; Yale University press: New Haven, **1967**.
10. Hon D., Chemical modification of lignocellulosic materials; Marcel Dekker Inc.: New York, **1996**, 36.
11. Ranby G., The colloidal properties of cellulose micelles. *Discussions Faraday Society* **1951,** 11, 158-164.
12. Millet M; Moore W; Saeman J., Preparation and properties of hydrocellulose. *Industrial Engineering Journal* **1954,** 46, 1493-1497.
13. Dong X; Revol J; Gray D., Effect of microcrystallite preparation conditions on the formation of colloid crystals of cellulose. *Cellulose* **1998,** 5, (1), 19-32.
14. Crank J; Park G., Diffusion in polymers; Academic Press: New York, **1968**, 1-40.
15. Finch C., Polyvinyl alcohol developments; John Wiley & Sons: New York, **1992**.
16. Arndt K; Richter A; Ludwig S; Zimmermann J; Kressker J; Kuckling D; Alder H., Poly(vinyl alcohol)/ poly(acrylic acid) hydrogels: FT-IR spectroscopic characterization of crosslinking reaction and work at transition point. *Acta Polymers* **1999,** 50, 383-390.
17. Kumeta K; Nagashima I; Matsui S; Mizoguchi K., Crosslinking reaction of poly(vinyl alcohol) with poly(acrylic acid) by heat treatment: Effect of neutralization of PAA. *Journal of Applied Polymer Science* **2003,** 90, 2420-2427.
18. Sanli O; Asman G., Release of diclofenac through gluteraldehyde crosslinked poly(vinyl alcohol) / poly(acrylic acid) alloy membranes. *Journal of Applied Polymer Science* **2003,** 91.

19. Donahue K., Chemical and biological barrier materials for collective protection shelters. *http://nsc.natick.army.mil/jocotas/ColPro_Papers/Donahue.pdf*, **2004**.

Morphology, mechanical and thermal properties of Poly(vinyl alcohol) / Cellulose Nanocrystal Barrier Films.

Shweta Paralikar and Dr. John Simonsen

Abstract

There is a continual interest in developing robust, flexible, durable, lightweight, waterborne polymer barrier coatings which are increasingly resistant towards both chemical warfare agents as well as an ever growing number of toxic industrial chemicals. In this study, barrier films were prepared with poly(vinyl alcohol) (PVOH) and different amounts of cellulose nanocrystals (CNXLs) as filler. Poly(acrylic acid) (PAA) was used as a crosslinking agent to provide water resistance to PVOH. The films were heat treated at various temperatures (125, 150, 170, 185 °C) in order to determine the optimimum crosslinking density. Heat treatment at 170 °C for 45 minutes resulted in films with improved water resistance without polymer degradation. Infrared spectroscopy (FTIR) indicated ester bond formation with heat treatment. Mechanical tests showed that films with 10%CNXLs/ 10%PAA/ 80%PVOH had the highest tensile strength, tensile modulus and toughness of all the films studied. Polarized optical microscopy and atomic force microscopy showed agglomeration of CNXLs at filler loadings of 20% CNXLs. Differential thermogravimetric analysis (DTGA) showed highly synergistic effects with 10%CNXLs/ 10%PAA/ 80%PVOH and supported the tensile test results. Barrier properties will be discussed in a future publication.

Introduction

The field of polymer nanocomposites is a rapidly expanding area of research generating new materials with novel properties.[20] Several new materials have been

developed within the last decade incorporating nanosized filler material in polymer matrices. Use of nanomaterials has proven to confer various advantages like improved mechanical, thermal and barrier properties compared to nonfilled polymers. These effects are largely due to their high interfacial area, their aspect ratio, their extent of dispersion and percolation, which occurs when the filler particles are present in quantities above the threshold where they start interacting.[21] Nanomaterials, e.g. glass fibers, carbon nanotubes, exfoliated clay, and cellulose nanocrystals have been successfully employed as fillers in polymer matrices and some systems are being commercialized.[22, 23]

One application area for these materials is barrier films, where the nano-sized fillers impart enhanced mechanical and barrier properties. Research in this area is evolving rapidly to enhance the barrier properties and to overcome certain limitations, e.g. durability, weight, robustness, flexibility and packing volume. Superior barrier films find their use in food and biomedical packaging where low permeability to oxygen, aromas, oils, or water are needed.[24, 25] The most extensively used filler nanomaterial is highly exfoliated clay, whose high surface area provides beneficial barrier and mechanical properties.[26, 27] Films with good thermal resistance and stiffness were obtained with the introduction of <5% clay in polymer matrices such as polyester, polyimide, polypropylene, poly(ethylene terephthalate) and poly(vinyl chloride).[26, 28, 29, 30, 31]

While most barrier films are designed to prevent the permeation of hydrophilic substances, such as water, there are certain situations where reducing permeability to

hydrophobic substances is important. One such area is barrier films for chemical warfare agents, which are mostly hydrophobic.[32] In this case, the most effective material is likely to be a hydrophilic filler. Nanocrystalline cellulose holds promise as a filler material for this application. It has the potential to provide improved mechanical, physical and barrier properties to hydrophobes in polymeric matrices.

Recently, cellulose nanocrystals (CNXLs) have attracted much attention from researchers for their remarkable reinforcing abilities.[33, 34, 35] Cellulose fibers are easily obtained from biomass and are an abundant, renewable, biodegradable resource. Nanocrystalline cellulose is the crystalline portion obtained after acid hydrolysis of cellulose. Some advantageous properties of CNXLs are their high aspect ratio of around 30-150 (length/width), low density of around 1.56 g/cc, high elastic modulus and strength reported to be 145 GPa[35, 36, 37] and 7500 MPa respectively.[38] Orts et al.[33] obtained cellulose from various sources and added low concentrations in polymer blends to study the reinforcement effect of cellulose. They found 10.3 % cellulose fibril content increased the Young's modulus by five fold in an extruded starch thermoplastic. They observed complex interactions between the components.

Two major disadvantages with using cellulose as nanofiller are agglomeration due to high hydroxyl content and dispersion of cellulose in the polymer matrix, especially in a hydrophobic matrix. Surface compatibility by physical or chemical treatment is required when composites are prepared with cellulose and hydrophobic polymers.[34] Zimmermann et al.[35] dispersed cellulose fibers in the hydrophilic polymers poly(vinyl alcohol) and hydroxypropyl cellulose to study their reinforcing

effect. Mechanical tests conducted showed a three fold increase in Young's modulus and a five fold increase in tensile strength compared to the base materials. The elongation at rupture increased 500% with 5 wt% of the fibrils and 300% at 10 or 20 wt% of the cellulose compared to the pure polymer. Borges et al.[39] studied the addition of coupling agent 1,4-butyl diisocyanate, which improved the interaction between cellulose and hydroxypropyl cellulose. With a coupling agent the yield stress increased slightly, the rupture stress and Young's modulus almost doubled while the % elongation decreased by 10% for films with 10 wt% cellulose fibers. Heat treating the same film further increased the rupture stress and yield stress by 50% while Young's modulus and % elongation did not improve significantly.

Poly(vinyl alcohol) (PVOH) has been extensively studied as a controlled drug release hydrogel, membrane material for chemical separations, barrier films for food packaging, pharmaceuticals, manufacturing artificial human organs and as a biomaterial.[40, 41, 42, 43, 44] It is resistant to permeation of solvents and oils and acts as a good barrier against oxygen and aroma. Since PVOH is a hydrophilic polymer, dispersion of hydrophilic CNXLs into the matrix can be successfully achieved by blending a PVOH solution with a CNXL dispersion. However, PVOH films have poor stability in water unless crosslinked [45, 46] because the water molecules swell the polymer and disrupt its barrier properties. Crosslinking can be achieved by agents that bind with the hydroxyl groups or by controlled heat treatment.[40, 47]

Crosslinking with monoaldehydes and dialdehydes has been successful to provide water resistance to PVOH, but the process is not cost effective and it leaves

undesirable toxic crosslinking agents.[47] Heat treatment, a low cost method to provide insolubility to films, provides crystallanity within PVOH matrices at 200 °C and 10 min treatment time.[48] Temporary insolubility is achieved when PVOH fibers are heat treated with drawing.[45] Another method for crosslinking is by repeated freeze/thaw cycles of PVOH gels, which forms physically crosslinked PVOH with a three dimensional network. These gels are mechanically strong, but their long term stability is an issue.[47] Poly(acrylic acid) (PAA) has been successfully used as a chemical crosslinking agent for PVOH.[45] The PVOH/PAA combination has been studied as a hydrogel for biomedical applications[49] and as a separation membrane material.[50] The amount of PAA added creates a highly networked structure and different mesh sizes can be obtained. By controlling the mesh size the size of molecules that can pass through the membrane is controlled.[51] A blend with PVOH/PAA ratio of 80/20 showed the best separation results for a methanol-water pervaporation separation membrane.[52] For an acetic acid–water pervaporation separating membrane a ratio of 75/25 (v/v) was found to be optimum with 40 °C as the optimum temperature.[50] Kumeta et al.[45] showed that using partially neutralized PAA in the range of 5-10 mol % along with heat treatment gives enhanced crosslinking reaction PVOH and PAA.

In this work, crosslinking was accomplished by using heat treatment and adding PAA as a crosslinking agent. The carboxyl group in PAA and the hydroxyl groups of PVOH and CNXLs formed ester linkages along with presumed hydrogen bonding between PVOH and CNXLs. This allows the overall nanocomposite to have

effective crosslinking and barrier resistance. The goal for these barrier films is to have the ability to prevent permeation of harmful chemicals and to be chemically inert, mechanically strong and tough, flexible and water resistant. While the ultimate application of the films studied herein is as chemical barriers, this paper reports the initial investigations on the system of PAA and CNXLs in PVOH. Mechanical properties, thermal properties and water solubility are reported. Significant improvements in performance were observed. A report on the barrier properties of these films is forthcoming.

Materials and Methods

Materials.

Poly (vinyl alcohol), (99 + % hydrolyzed, M_w = 89,000- 98,000) was obtained from Sigma-Aldrich, Inc (St Louis MO, USA). Poly(acrylic acid), (Mw = 2,000) was obtained from Aldrich Chemical Company, Inc (Milwaukee WI, USA).

Preparation of the solutions / dispersion.

5 wt % solutions of PVOH and PAA were prepared by dissolving the powder form in DI water and stirring in an oil bath at 85 °C for 30 min. Cellulose nanocrystals (CNXLs) were prepared in our laboratory from cotton (Whatman #1 filter paper), which was obtained from the Whatman Company (Clifton, NJ). Briefly, CNXLs were obtained by partial hydrolysis of ground filter paper with 65 % H_2SO_4 (v/v) solution at 45 °C with medium stirring for 50 minutes. The ground paper to acid

ratio was 1:10 g/mL. The mixture was centrifuged 5 times with DI water to remove the acid. The suspension was then subjected to ultrasonic irradiation in a Branson Sonifier (Danbury, CT) for 15 minutes to disperse the CNXLs and break any agglomerates formed. The suspension was next ultrafiltered to remove salts until the conductivity was <10 μS/cm. The dispersed CNXLs were then concentrated in a Rotavaporizer R110 (Buchi, Flawil, Switzerland) to obtain an aqueous dispersion of 1% CNXLs.

Preparation of the films.

Stock solutions were prepared by blending a calculated volume of the components with the required wt % solids. Before casting, the solutions were sonicated for 25 minutes to re-disperse any agglomerates formed. The thickness of the film was controlled by pouring a known volume of the blend solution into a flat-bottomed plastic dish. The films were formed by air drying for 48 hrs. Within the films, the CNXL content was varied from 0-20 wt % in increments of 5 wt % and the PAA content was varied from 0-20 wt % in increments of 10 wt % with the remainder of the content being PVOH. The obtained films were heat treated in a convection oven at specified times and temperatures.

Heat treatment optimization.

Swelling and Dissolution.

The cast films were weighed (Weight 1) and submerged in deionized water at room temperature. The films were periodically removed, wiped dry with a tissue to

remove any surface water and weighed (Weight 2). Next, the films were dried in an oven at 40 °C until a constant weight was obtained (Weight 3). For each soaking cycle, the % swelling and % solubility were calculated as follows

$$\%\ Swelling = \frac{(Weight\ 2 - Weight\ 3)}{Weight\ 3} * 100\ \%$$

$$\%\ Solubility = \frac{(Weight\ 1 - Weight\ 3)}{Weight\ 1} * 100\ \%$$

Fourier Transform Infrared Spectroscopy (FTIR).

FTIR analysis was performed using a Nexus 470 FTIR spectrometer (Thermo Nicolet, Madison, WI) in an absorbance range of 4000-500 cm^{-1}, to compare the non-heat treated and the heat treated films. Films with 10 μ thickness were cast for observation. Since pure PAA is too brittle to be formed into a film, pellets formed with PAA and KBr powder were used for this observation. The charts obtained were automatic baseline corrected and brought to a common scale for comparison.

Material Properties.

Mechanical Testing.

A universal testing machine Sintech 1/G (MTS, Cary, NC) was used for mechanical testing in tensile mode. The heat treated films of 25-27 μm thickness were cut into a dogbone shape using a cutter. Each test was replicated thrice. The

crosshead speed was maintained at 1 mm/min with an initial span of 20 mm. Four properties were determined from the obtained load vs. elongation curves 1) tensile strength, 2) tensile modulus, 3) elongation at break and 4) work to failure (toughness). The tensile strength was the yield load divided by the initial cross sectional area of the specimen. The modulus was obtained as the slope of the initial linear portion of the curve. The elongation at break was obtained as % elongation by dividing the extension by the initial span. The value for toughness was obtained as the area under the load vs. elongation curve.

Thermal Analysis.

A modulated TGA 2950 thermogravimetric analyzer (TGA) (TA instruments, Newark, DE) was used to test the thermal degradation of the composite films. The temperature was ramped from room temperature to 600 °C at a heating rate of 20 °C/min under nitrogen. Differential thermogravimetric analysis (DTGA) curves were obtained from the TGA data by differentiating the later with respect to temperature ($-\partial W/\partial T$).

Quality of dispersion.

Atomic force microscopy (AFM).

A Dimension 3100 atomic force microscopy (AFM) (Veeco Instruments, Santa Barbara, CA) in tapping mode was used to observe the dispersion of the CNXLs

within the film. The film sample was embedded in epoxy and microtomed by a diamond knife to expose the cross section.

Scanning electron microscopy (SEM).

The morphology of the films was characterized with a scanning electron microscope (SEM) AmRay 3300FE (AmRay Inc, Bedford, MA) to study the fracture behavior. The films were fractured under liquid nitrogen. The fractured surfaces were mounted on aluminum mounts, PELCO # 16262. The samples were sputter coated with 60/40 wt% gold/palladium alloy in an EDWARDS S 150B sputter coater.

Polarized optical microscopy (POM).

Images were obtained with a Photometrics Cool Snap (Roper scientific, Tuscon, AZ) attached to an Eclipse E400 Nikon microscope (Nikon Company, Melville, NY) using crossed polarizers.

Results and Discussion

Water dissolution test.

The first set of experiments, which was the water dissolution test, was intended to optimize the heat treatment procedure by minimizing the % solubility and % swelling. At 185 °C for 60 min the film samples exhibited a light brown coloration indicating degradation so this temperature was discontinued for further tests. The samples heat treated at 125 °C for 60 min completely disintegrated with water immersion after a few hours, while the samples heat treated at 150 °C for 60 min and

170 °C for 60 min did not. This suggested improvement of the crosslinking density with the increase in heat treatment temperature. The time for heat treatment was reduced to 45 minutes as the films assumed a light yellow coloration with 170 °C for 60 min heat treatment condition. The increase in heat treatment temperature from 150 °C for 45 min to 170 °C for 45 min clearly decreased the total %solubility in each blend composition of the film (Figure 2.1). Thus, the optimum heat treatment was chosen as 170 °C for 45 min.

The addition of PAA reduced the total % solubility greatly (Figure 2.1), suggesting a decrease in the unreacted PVOH molecular chains, which would otherwise leach out in the water. The total % solubility of the films containing 20% PAA was just 1.3%, which was presumably due to the highly crosslinked matrix with a networked structure. However, this film was very brittle.

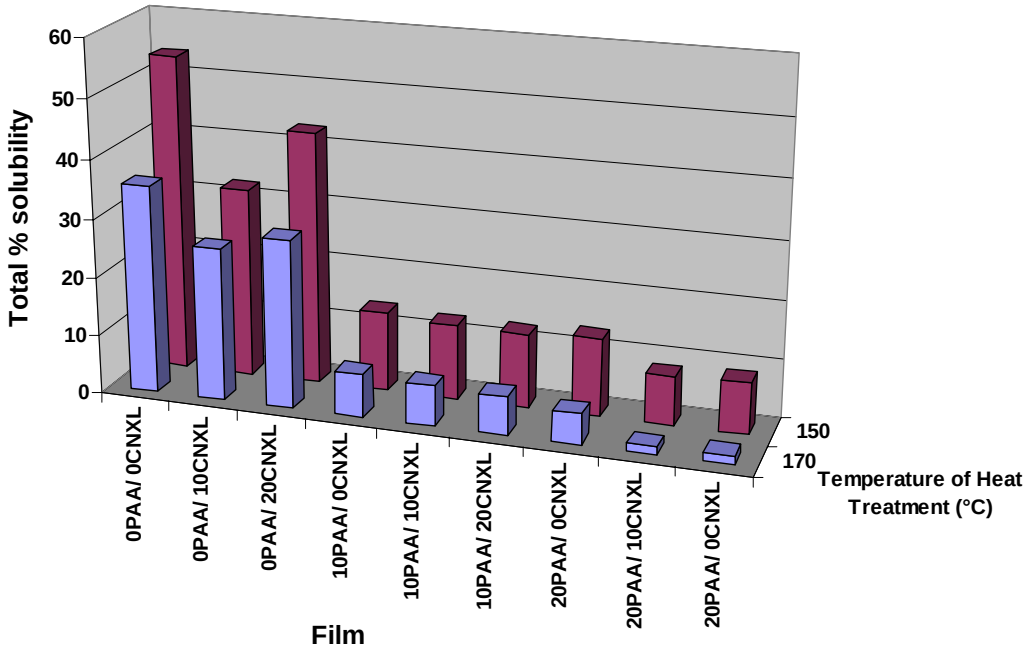

Figure 2.1. Total % solubility after 72 hours of heat treatment at 150 °C and 170 °C for 45 minutes. PAA = wt % Poly(acrylic acid), CNXL= wt % cellulose nanocrystals.

The addition of CNXLs in the presence of PAA did not cause a great difference in the % solubility. Evidently, if CNXLs were forming any hydrogen bonds with PVOH they were easily broken in the presence of water.

Fourier transform infrared spectroscopy (FTIR).

The presence of crosslinking was investigated using FTIR. 10%PAA/ 10%CNXLs/ 80%PVOH film showed a broad carbonyl peak at 1715 cm^{-1}, which upon heat treatment shifted to1723 cm^{-1} along with the disappearance of the shoulder at 1700-1600 cm^{-1} (Figure 2.2A). Compared to the stable methylene peak at 2920 cm^{-1} the absorbance of OH peak at 3300-3400 cm^{-1} reduced.

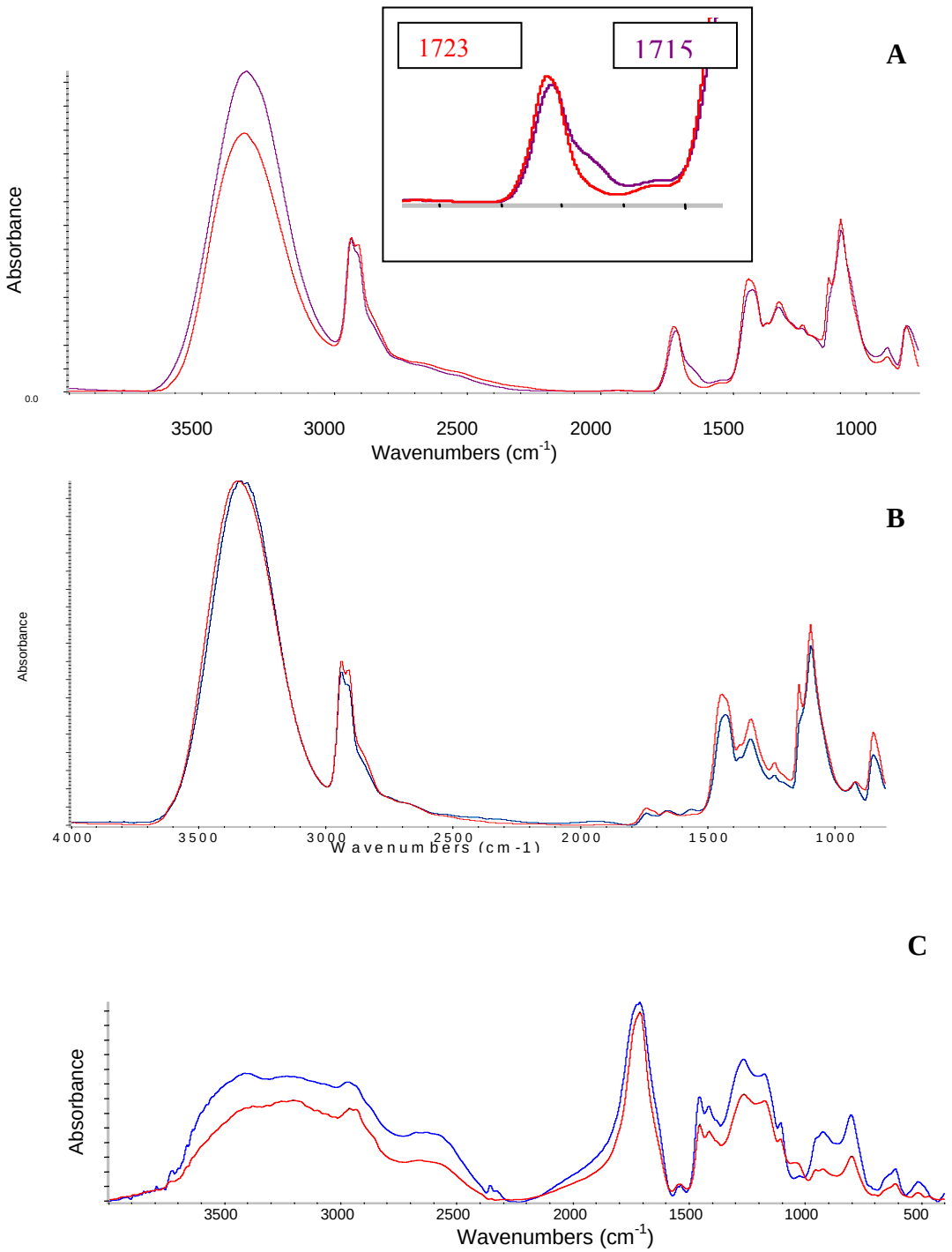

Figure 2.2. FTIR spectra of (A) 10 % PAA/ 10 % CNXLs/ 80 % PVOH. (B) 100 % PVOH film. (C) 100 % PAA film. Blue: Non heat treated, Red: Heat treated.

An FTIR of pure PVOH heat treated for 45 minutes at 170 °C showed that the absorbance of the OH peak at 3300-3400 cm $^{-1}$ remained the same, indicating that the carbonyl peak did not originate from ketone formation by degradation of PVOH (Figure 2.2B). FTIR spectra of pure PAA were obtained to see if the position of the carbonyl peak of PAA shifted with heat treatment. No such shift was observed in the FTIR spectrum of pure PAA (Figure 2.2C). Therefore, it was concluded that the peak at 1723 cm $^{-1}$ (Figure 2.2A) and the reduction of OH peak at 3300-3400 cm $^{-1}$ was due to the formation of carboxylic esters formed by the heat treatment. The shoulder at 1700-1600 cm^{-1} is unassigned at present, but probably arises from oxidation of the CNXLs during hydrolysis while the CNXLs are being produced. We speculate that heat treatment may then further oxidize these groups to caroboxylic acid.

Swelling test.

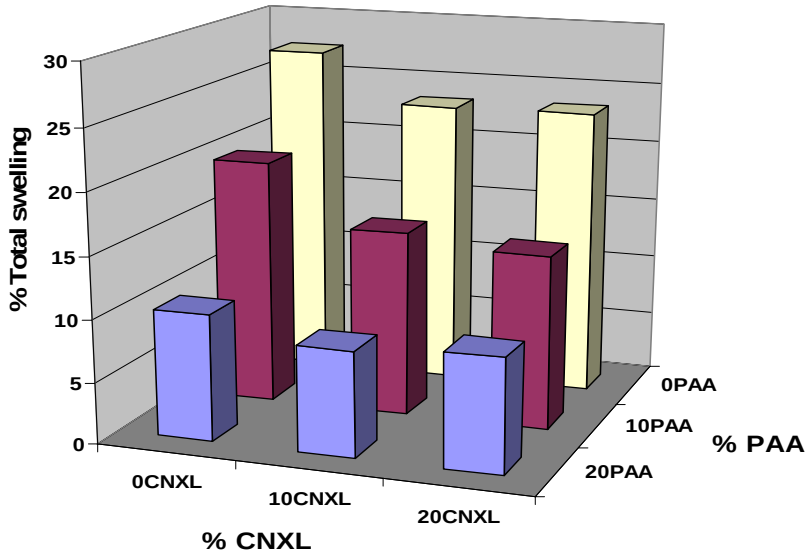

Figure 2.3. Total % swelling, after 72 hours of soaking time, for films with heat treatment at 170 °C for 45 min.

The total % swelling decreased dramatically with increasing PAA content and slightly with increasing CNXL content (Figure 1.3). With the heat treatment the polymer chains were interconnected with ester linkages and the chain mobility was reduced, reducing swelling. Results with the addition of 20% CNXLs showed an increase in swelling compared to 10% CNXLs, which was possibly due to agglomeration of the CNXLs and the consequent formation of a separate CNXL phase and reduced CNXL content in the matrix.

Polarized optical microscopy.

Since, cellulose is crystalline it rotates light and thus appears bright between crossed polarizers. The films with 5% (Figure 2.4A) or 10 % CNXLs (Figure 2.4B) showed good dispersion of the CNXLs while higher CNXL contents showed obvious agglomeration (Figure 2.4C).

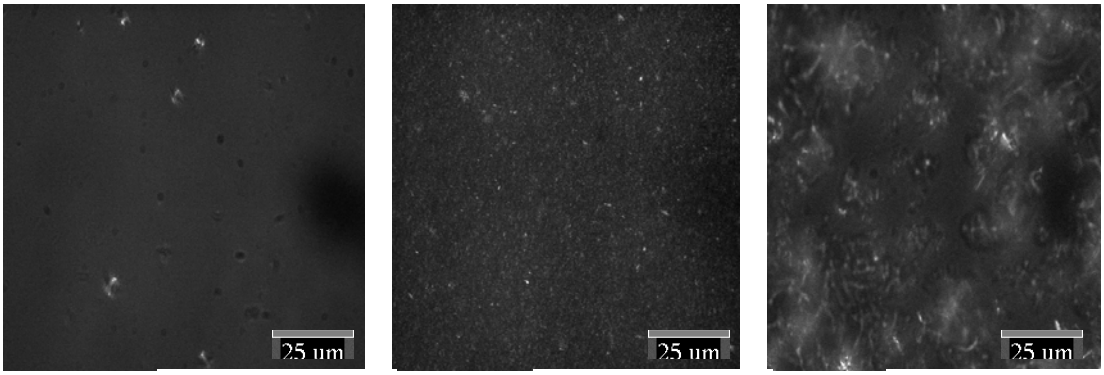

Figure 2.4. Polarized optical microscopy pictures with (A) 5 wt % CNXL/ 10 wt %PAA. (B) 10 wt % CNXL/ 10 wt % PAA. (C) 15 wt % CNXL/ 10 wt % PAA and PVOH makes up the remaining content of the films.

Mechanical properties.

Filled nanocomposites have been shown to improve both tensile modulus and elasticity.[33, 34] With the addition of 10% PAA and 10% CNXLs to PVOH the ultimate tensile strength (UTS) shows a 150 % improvement as compared to pure PVOH (Figure 2.5A).

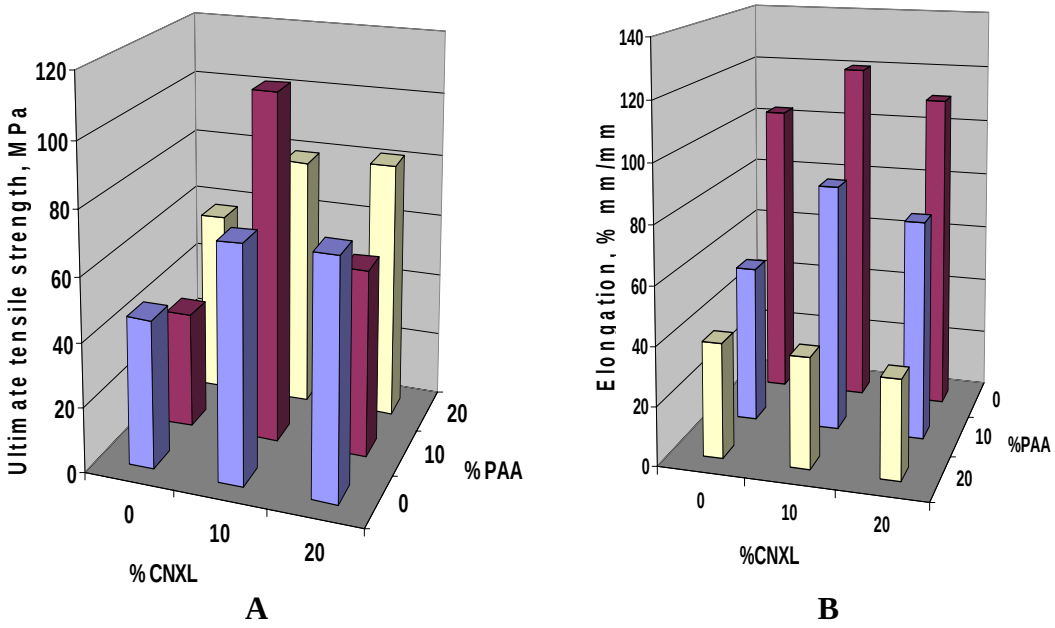

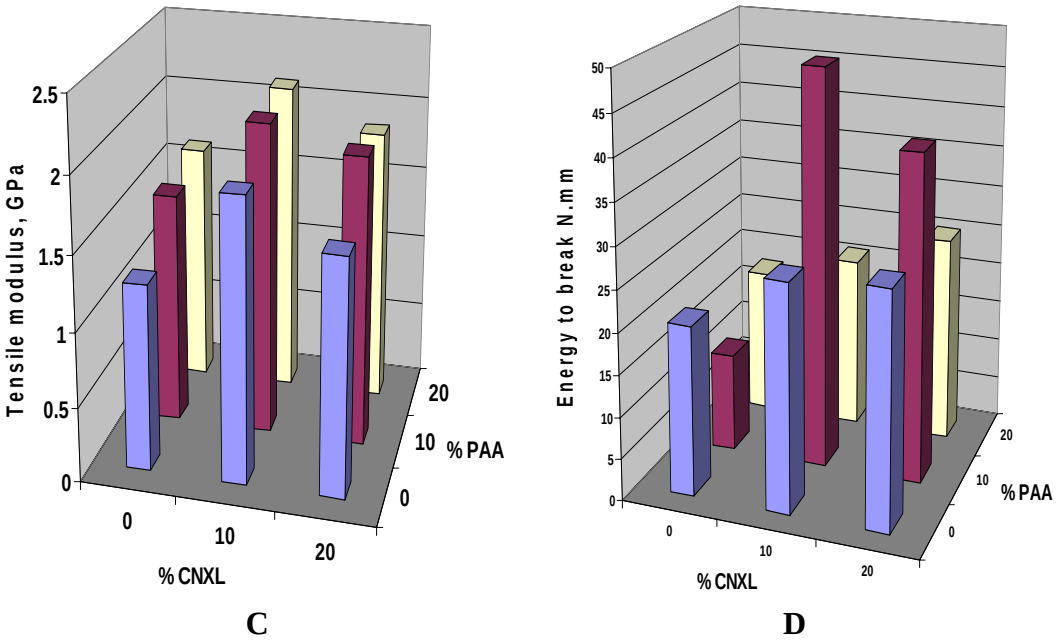

Figure 2.5. Sintech tensile test charts. (A) Ultimate tensile strength. (B) % Elongation. (C) Tensile modulus. (D) Energy to break (Toughness).

The coefficient of variation obtained was 3.5 – 6.2 %. The changes in UTS with either CNXL or PAA content were not linear. A large synergistic increase was observed with the 10% CNXL/ 10% PAA sample. Otherwise, UTS appeared to increase with CNXL content (with the exception of the 10% PAA series). Increasing PAA content did not show any consistent trend in UTS. Elongation increased with CNXL content in the absence of PAA (Figure 2.5B). The coefficient of variation obtained was 5.2-8.9 %.

While polymer composites are known to show increases in elongation with low filler loadings[33], the behavior observed here is unusual and suggests a close association between the PVOH and CNXLs in the films. The addition of PAA adds to brittleness in the films as expected. In fact, the films containing 20% PAA showed a

70% reduction in elongation compared to pure PVOH film. The films with 20% PAA were brittle and were excluded from further tests.

The tensile modulus increased with the addition of CNXLs from 0% to 10%, but then dropped (Figure 2.5C). The coefficient of variation obtained was 6-9.5%. We speculate that the drop in modulus with CNXL content was due to agglomeration. Modulus increased with PAA content from 0% to 10%, then leveled off. This suggested that either there was no additional crosslinking in the 20% PAA sample compared to the 10%, or that the 10% already had sufficient crosslinking to maximize the modulus. Again, we see a significant synergy for the 10% CNXL/ 10% PAA sample.

The energy to break is the area under the stress strain curve, which is one measure of the toughness of the material. A significant synergy was observed once again with the 10% CNXL/ 10% PAA sample (Figure 2.5D). The coefficient of variation obtained was 4-9.5%. With an increase in the PAA content to 20% the brittleness in the films increased, the % elongation decreased and as a result toughness decreased. Overall, the films with 10% PAA, with either 10 or 20% CNXLs, showed excellent toughness. Again, 10% PAA with 10% CNXLs showed excellent toughness with 2.5 times improvement in UTS and twice the tensile modulus compared to pure PVOH.

Atomic force microscopy (AFM).

The pure PVOH film appeared flat and featureless in AFM image (Figure 2.6A). Since cellulose is crystalline and hard it gives a structured phase image (Figure 2.6B).

With 10% CNXLs in the film the nanoparticles were observed as small features. The extent of agglomeration was difficult to discern from these images since the CNXLs were not being directly imaged, but only their effect on the surface of the film in tapping mode. A film with 20% CNXLs showed highly agglomerated CNXLs in the top half of the scanned surface, with remainder of the surface observed consisting of matrix (Figure 2.6C). This supports the observation from polarized optical microscopy that the CNXLs were agglomerated in these samples.

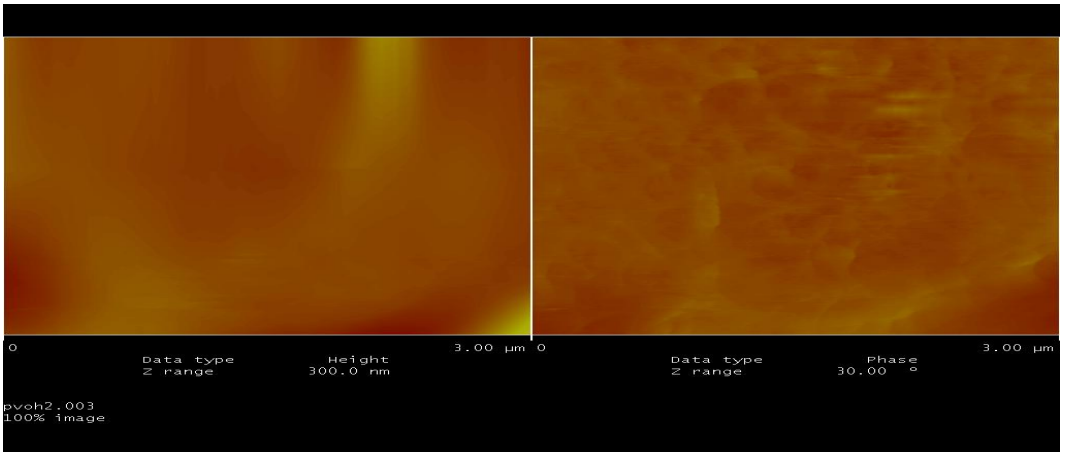

A

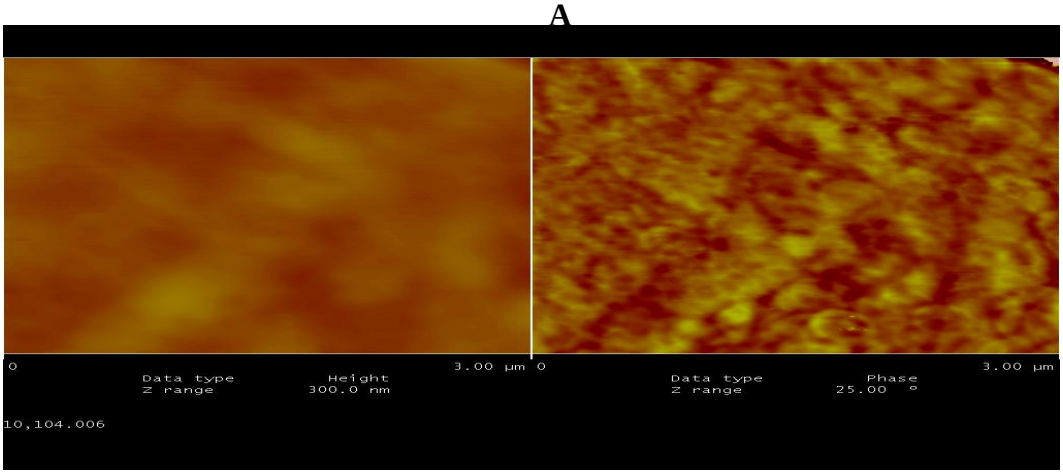

B

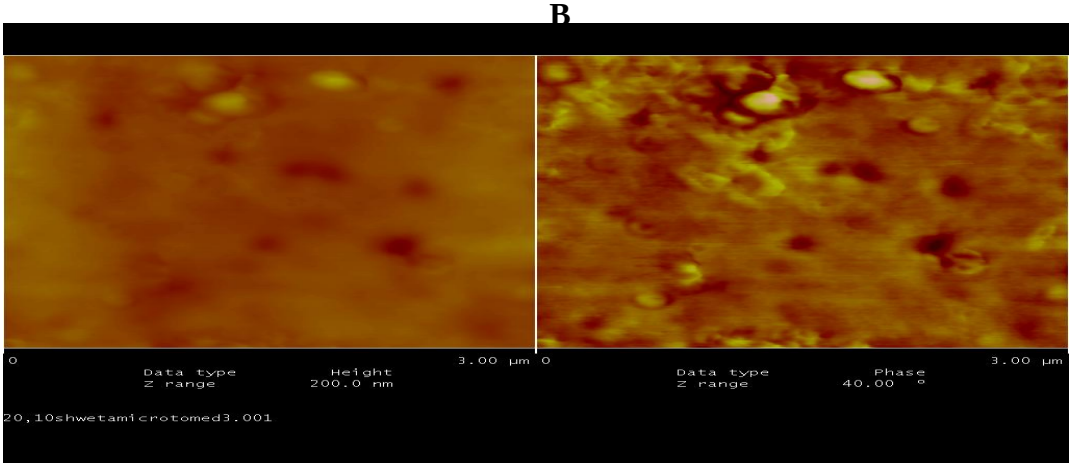

C

Figure 2.6. Images from AFM in tapping mode. Right side represents the phase image while left side is the height image. (A) 100 % PVOH film. (B) 10 % PAA/ 10% CNXLs/ 80% PVOH. (C) 10 % PAA/ 20% CNXLs/ 70 % PVOH.

Scanning electron microscopy (SEM).

The SEM of the fractured surface showed a smooth fractured surface for 100% PVOH (Figure 2.7A). A rough texture with small cracks was observed in the presence of CNXLs and PAA (Figure 2.7B).

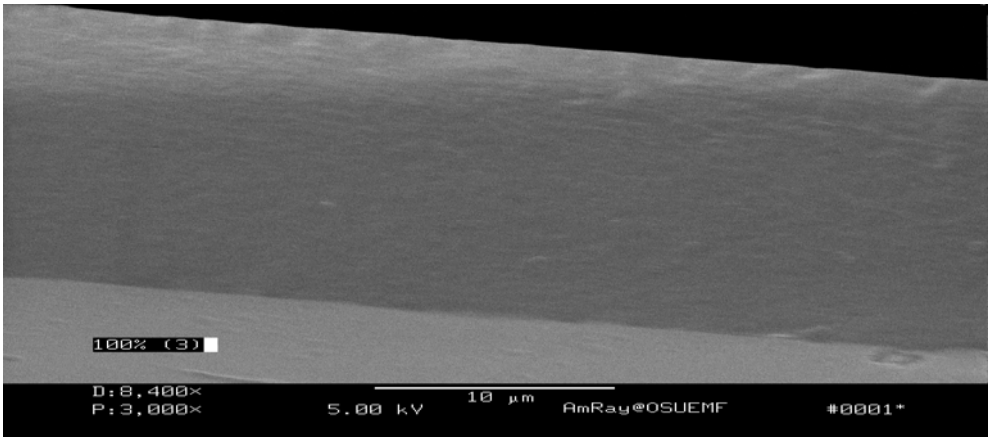

A

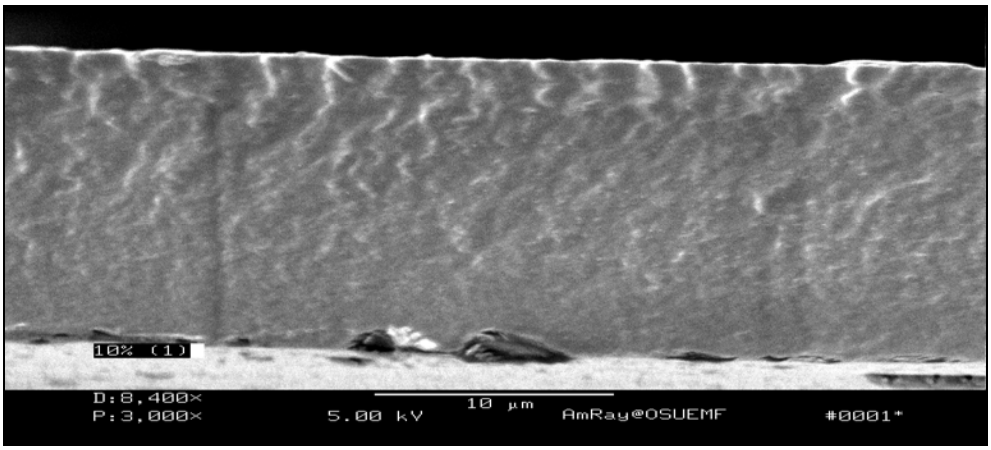

B

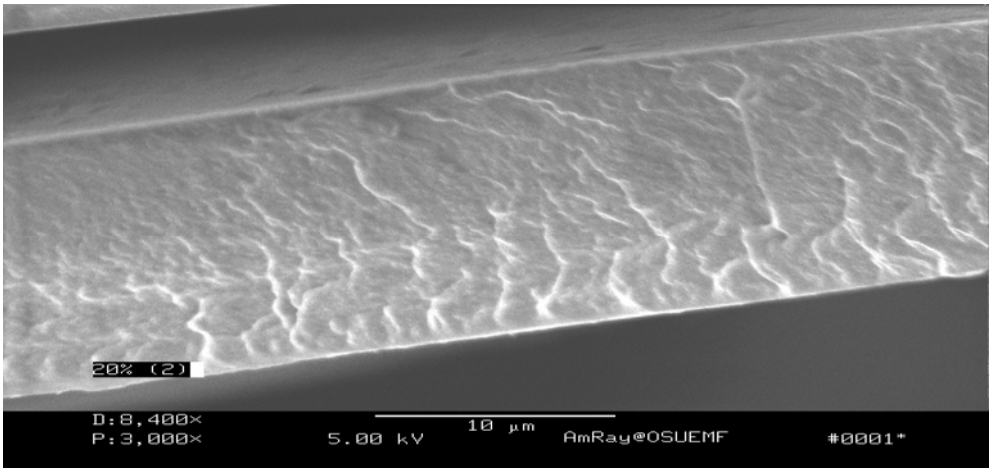

C

Figure 2.7. Fractured surface images by SEM. (A) 100 % PVOH (B) 10 % PAA/ 10% CNXLs/ 80% PVOH (C) 10 % PAA/ 20% CNXLs/ 70 % PVOH.

The fracture initiated the crack formation but well dispersed CNXLs and good bonding between the components evidently prevented further crack proliferation. The rough texture could be attributed to the addition of PAA which added to the stiffness of and brittleness of the films. Films with CNXL contents > 10 wt % showed more cracks which were deeper, wider and longer (Figure 2.7C). Supporting the optical microscopy results, CNXLs were found to be agglomerated in the 20% samples. Within these agglomerates the interaction with the matrix is poor and the resistance to separation is poor, hence crack propogation is enhanced.

Thermal gravimetric analysis.

Pure PAA and pure PVOH degraded thermally in three steps (Figure 2.8A).

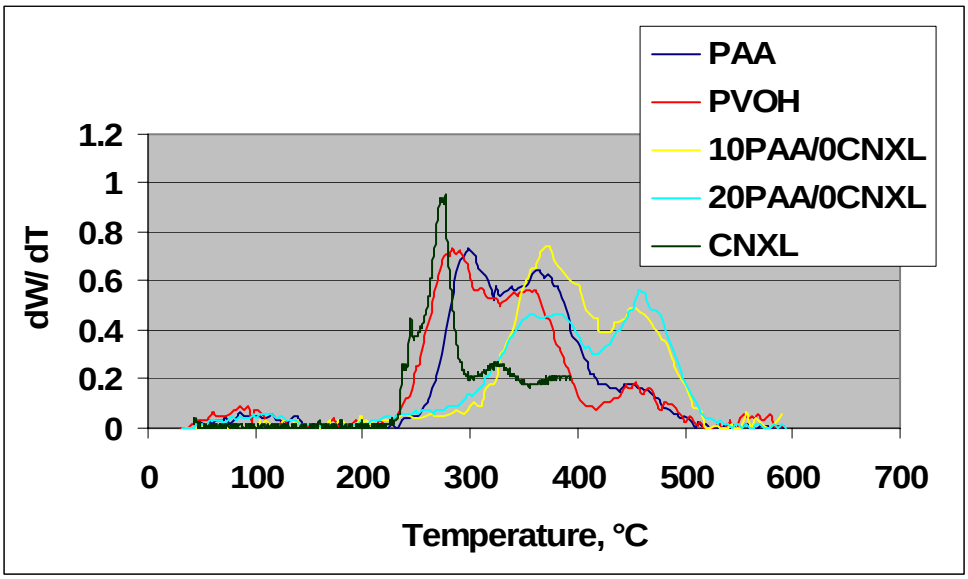

A

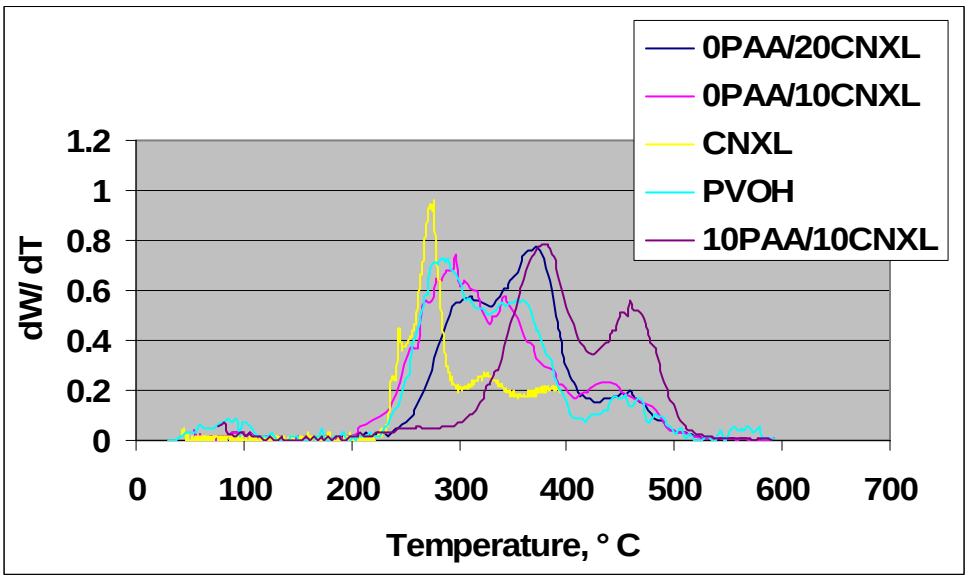

B

Figure 2.8. DTGA graphs showing the thermal degradation of selected films. (A) Data with no CNXLs are compared to the pure components (PVOH, PAA and CNXLs). (B) Data with no PAA are compared with 10 % PAA/ 10 % CNXLs/ 80 % PVOH.

For pure PVOH, the maxima occurred at 290 °C, 347 °C and 454 °C. The maxima for pure PAA occurred at 300 °C, 360 °C and 454 °C. When PVOH and PAA were blended together only two maxima were observed and they shifted to higher temperatures at 374 °C and 463 °C. This suggests bonding between PVOH and PAA molecular chains. Pure CNXL started degrading at 220 °C with its maxima at 273 °C. Data for the pure CNXL graph was obtained from thesis of Yong jae Choi, 2005.[53] Various blends of PAA, CNXL and PVOH with 10 -20% of PAA or CNXL were observed to be similar to the DTGA graph of 10%PAA/ 10%CNXL and are therefore not shown.

Blends with no PAA were compared with 10%PAA/ 10%CNXL/ 80%PVOH film (Figure 2.8B). Films with no PAA degraded in a three step mechanism. We conclude the presence of PAA plays an essential role in creating interactions within the blend composite. While PVOH degraded with a three step mechanism, we see just three degradation steps in blends of PVOH and CNXLs suggesting close association between PVOH and CNXLs as well. Overall, the film with 10%PAA/ 10%CNXL/ 80%PVOH does not loose its integrity as a composite material and this combination holds promise for its further development as a barrier film.

Conclusions

Heat treatment improved the crosslinking density within the films made of varying contents of CNXL, PAA and PVOH. Solubility results indicate that higher temperature results in higher crosslink density within the matrix. The FTIR spectrum indicates heat treatment results in formation of ester linkages between PAA and

PVOH. CNXLs were well dispersed in blend films of PVOH and PAA at 10 % content by weight, but agglomerated at 20%. This result is supported by AFM and optical microscopy images. The presence of CNXLs and crosslinking almost doubles the strength, stiffness and toughness, while the elongation is reduced by 20%. The DTGA suggests close association between PVOH and CNXL without the presence of PAA. The DTGA result supports the synergistic effect of 10% CNXLs and 10% PAA in a PVOH matrix. This combination holds promise and will be tested further for its barrier properties.

Acknowledgement

We gratefully acknowledge the support from the National Research Initiative of the USDA Cooperative State Research, Education and Extension Service, grant number 2003-35103-13711

Surface modification and barrier properties of Cellulose Nanocrystal/ Poly(vinyl alcohol) Films.

Shweta Paralikar, John Simonsen

Abstract

Previous work to develop improved waterborne polymer barrier coatings (Chapter 2) showed that films with 10% cellulose nanocrystals (CNXLs)/ 10% polyacrylic acid (PAA)/ 80% poly(vinyl alcohol) (PVOH) had the highest tensile strength, tensile modulus and toughness of all the films studied. Morphology and differential gravimetric analysis also indicated well dispersed CNXLs and highly synergistic effects at a filler loading of 10% CNXLs. This paper presents the water vapor diffusion, barrier properties as well as the effects of surface modification of the CNXLs. The purpose of these barrier films is to prevent the permeation of chemical warfare agents while allowing moisture to pass through to allow breathability. Water vapor transmission studies indicated that all the films allowed moisture to pass. Moisture diffusion was reduced by the presence of both CNXLs and PAA. The crystalline nature of CNXLs caused the diffusing molecules to undergo a tortuous path, while crosslinking formed a network structure which reduced diffusion. A standard time lag diffusion test utilizing permeation cups was used to study the chemical barrier properties. The film containing 10%CNXL/ 10%PAA/ 80%PVOH showed an improvement in time lag of 90% compared to the control. Surface modification of CNXLs was successful and well dispersed carboxylated CNXLs were obtained. Carboxylated cellulose nanocrystals (C.CNXLs) showed less agglomeration, improved interaction, slightly reduced flux and slightly increased time lags compared to CNXLs.

Introduction

The field of polymer nanocomposites is a rapidly expanding area of research generating new materials with novel properties.[20] One application area for these materials is barrier films, where the nano-sized fillers impart enhanced mechanical and barrier properties. Superior barrier films find their use in food and biomedical packaging where low permeability to oxygen, chemicals, aromas, oils, or water are needed.[24, 54] While most barrier films are designed to prevent the permeation of hydrophilic substances, such as water, there are certain situations where reducing permeability to hydrophobic substances is important. Barrier films for chemical warfare agents are mostly hydrophobic.[32] In this case, the most effective material is likely to be a hydrophilic filler. Nanocrystalline cellulose holds promise as a filler material for this application. It has the potential to provide improved mechanical, physical and barrier properties to hydrophobes in polymeric matrices.

Many barrier films have been developed to allow permeation of one chemical while restricting the permeation of others. An example is chemical protective clothing or films to prevent the passage of toxic chemicals while allowing moisture to pass through the films. Such films are used on tents or on clothing by the US military or in chemical industries where workers are exposed to toxic chemical vapors. Research in this area is evolving rapidly to enhance the barrier properties and overcome certain limitations like durability, robustness, flexibility, cost, weight, and packing volume amongst several others. These barrier films are typically coated on fabric material.

The use of coatings which contain nanofillers in a polymer matrix are solutions which show promise.[32] Typical chemical warfare agent barrier polymers currently employed include isobutylene rubber, vinylidene chloride (Saranex) polymers, highly crosslinked polyurethane (CARC paint), fluorocarbons and vinyl alcohol copolymers.[32]

This paper reports the barrier properties with the water vapor and chemical vapor transmission test. Significant synergy was observed in the barrier properties at the same film composition which showed optimal mechanical properties (see Chapter 2). Surface modification of the CNXLs was performed in an attempt to provide for more direct crosslinking between PVOH and CNXLs. While barrier property improvements were small, significant improvements in the mechanical and thermal properties were observed as a result of better dispersion.

Materials and Methods

Materials.

Poly(vinyl alcohol), (99 + % hydrolyzed, M_w = 89,000- 98,000) was obtained from Sigma-Aldrich, Inc (St Louis MO, USA). Poly(acrylic acid), (Mw = 2,000) was obtained from Aldrich Chemical Company, Inc (Milwaukee WI, USA).

Materials for carboxylation of CNXLs.

Sodium hypochlorite (NaClO) 6%, was obtained from VWR international (West Chester, PA, USA), Sodium bromide was from EM Industries Inc (Gibbstown,

NJ, USA) and 2,2,6,6 – tetramethyl-1-piperidinyloxy radical (TEMPO) was obtained from Sigma-Aldrich Inc. (St Louis, MO, USA).

Preparation of the solutions / dispersions.

Followed procedures previously published (Chapter 2).

Surface modification of cellulose nanocrystals.

200 mL of a 1% CNXL dispersion was mixed with 0.2 gm of TEMPO and 2 gm of NaBr. The oxidation reaction was initiated with the addition of 10 mL of NaClO solution. 10 mL NaClO was subsequently added after 2 and 4 hours. The overall reaction time was 15 hours and a pH of 10 was maintained throughout with the addition of 1N NaOH when necessary. The oxidation reaction was terminated by the addition of 30 mL of ethanol. The suspension was ultrafiltered thrice to remove unreacted reagents. A calculated amount of HCl was added to convert the carboxylate groups to free acid. The solution was again ultrafiltered until a conductivity of < 5 μS/cm was obtained. A dispersion with 1% carboxylated CNXLs was obtained by concentrating in a rotavaporizer R110 (Buchi, Flawil, Switzerland). Carboxylated content (mmols of acid group) of the dispersion was calculated by titrating against 0.01 N NaOH.

Preparation of the films.

Films were prepared using previously published methods (see Chapter 2), including the heat treatment at 170 °C/45 min.

Surface modification testing.

The films containing carboxylated CNXLs were evaluated using the same methods as previously reported (see Chapter 2).

Barrier Properties.

Water vapor transmission rate (WVTR).

For this test glass jars were half filled with water. The heat treated film was then glued over the glass jars. The films were all 26 μm thick. The initial weight of the assembly was noted. Three replicates of each sample were placed in a controlled environmental chamber at 30 °C and 30 % relative humidity. The weight change was noted after certain time intervals until a constant flux was obtained for three consecutive days, which gave the average flux. The water vapor transmission which was the average mass flux was obtained from the following equation.

$$J = \frac{M}{A * t}$$

Where,

J = Mass flux (g/ m^2 * day)

M= Weight change by loss of water in 24 hrs (g)

A = Area of the film available for mass transfer (m^2)

t = Time (day)

Chemical vapor transmission rate (CVTR).

CVTR was determined in accordance with ASTM Standard F 1407-99a (Standard method of resistance of chemical protective clothing materials to liquid permeation). A mustard gas simulant, 1,1,2 Trichloroethylene (TCE), was used for evaluation of the CVTR of the films. The film was clamped over the permeation cup, immediately weighed, inverted and stored in a chemical fume hood. Time and weight of the assembly was noted after certain intervals. A graph of total amount of solute transferred through the membrane at each sampling time, Q, was plotted against time. The linear portion of the curve obtained, when the flux becomes constant, was extended to intercept the x axis to obtain the breakthrough detection time (time lag). The slope of this line gave the value of flux (g/m^2 hrs) through the film. The time lag equation developed by Hannoun et al., [55] was used to calculate the diffusion coefficient and breakthrough detection time.

The assumptions made for the experimental setup were as follows: Mass transfer occurred in the z- direction only as the lateral directions were sealed. 2) The temperature and relative humidity of the system remained constant throughout the experiment. 3) A semi-steady state mass transfer occurred, where the flux became constant after a certain time interval. 4) The concentration of the simulant outside the film (C_2) was zero as it was swept away by the airflow in hood.

The diffusion process was thus governed by Fick's second law (Equation 1):

$$\frac{\partial C}{\partial t} = -D\,\frac{\partial^2 C}{\partial z^2} \qquad 1$$

Here,

C = Concentration of the simulant TCE,

D = Diffusion coefficient of TCE through the films,

t = Time,

z = The distance across the cross section of the film, i.e. the thickness of the film.

The boundary conditions were set up as follows, with the concentrations assumed constant on both the sides of the film:

$C = C_1$ at $z = 0$ $\quad t > 0$

$C = C_2$ at $z = l$ $\quad t > 0$

$C = 0$ at $t = 0$ $\quad 0 \le z \le l$

Where, $C = C_1$ is within the permeation cup directly in contact with the simulant and $C = C_2$ is on the outer side of the film in the atmosphere. Using the boundary conditions above and considering the initial concentration throughout the material to be zero, the analytical solution is given by Equation 2.[55]

$$C(z,t) = C1 + (C2 - C1)\frac{z}{l} + \frac{2}{l}\sum_{n=1}^{\infty}\frac{C_2\cos(n\Pi) - C_1}{n}.\sin\left(\frac{n\Pi z}{l}\right).e^{\left(\frac{-Dn^2\Pi^2.t}{l^2}\right)} \qquad 2$$

This equation can be differentiated and multiplied by the diffusion coefficient to give the instantaneous flux (J = -D ∂C/ ∂z). Integration of the flux with respect to time gives the cumulative amount of simulant Q(t) which passes the film at time t:

$$\mathrm{Q(t)} = \mathrm{D\,(C2\ -C1)}.\frac{t}{l} + \frac{2l}{\Pi^2}\sum_{n-1}^{\infty}\frac{C_1.\cos(n\Pi) - C_2}{n^2}.\left(1 - e^{\left(\frac{-Dn^2\Pi^2.t}{l^2}\right)}\right) \qquad 3$$

Since C2 = 0, Q (t) becomes,

$$\mathrm{Q(t)}\ = 1.\ \mathrm{C1}.\left(\frac{D.t}{l^2} - \frac{1}{6} - \frac{2}{\Pi^2}\sum_{n-1}^{\infty}\frac{(-1)^n}{n^2}.e^{\left(\frac{-Dn^2\Pi^2.t}{l^2}\right)}\right) \qquad 4$$

As t increases the exponential term becomes negligible and a steady state is attained where:

$$\mathrm{Q(t)} = \frac{DC_1}{l}\left(t - \frac{l^2}{6D}\right) \qquad 5$$

Extrapolating the linear portion of curve to the x-axis at Q=0, time lag can be obtained, from which the diffusion coefficient (D) is retrieved by using the following equation:

$$\mathrm{D} = \frac{l^2}{6.t_{timelag}} \qquad 6$$

Results and Discussion

Transport properties.

Water vapor transmission rate (WVTR).

Preferably, barrier films reduce/ retard the passage of chemical vapors while allowing moisture to pass through so that these films can be used on clothing. The transmission rates for pure PVOH films were taken as the control.

The flux decreased with the addition of PAA in the absence of CNXLs (Fig. 2.1). This is presumably because the carboxyl groups of PAA formed ester bonds with the available OH groups with the application of heat treatment forming a three dimensional network of reduced free volume which restricted the diffusion of water vapor. With the addition of CNXLs in the absence of PAA, the flux was reduced by more than 50% compared to the control (Fig. 3.1). This can be attributed to the tortuous path the water molecules have to travel around the CNXLs to diffuse through the film. Since, the filler material is crystalline it acts as a physical barrier to the transport of the diffusing molecules.[56] Furthermore, since CNXLs and PVOH both are hydrophilic in nature, the diffusing water molecules could be absorbed via hydrogen bonding, which would also alter the flux. Once a steady state equilibrium is attained, the flux remains constant and a three day average of these constant values are represented in the figure 3.1. The films with 10% CNXL show a lower flux than with 20% CNXL. This could be due to the better dispersion at lower CNXL content. With increased PAA content at 20 wt % there was no significant improvement in the flux

values. This was contradictory to what was expected by increasing the % PAA, which would provide more carboxyl bonds and thus greater crosslinking.

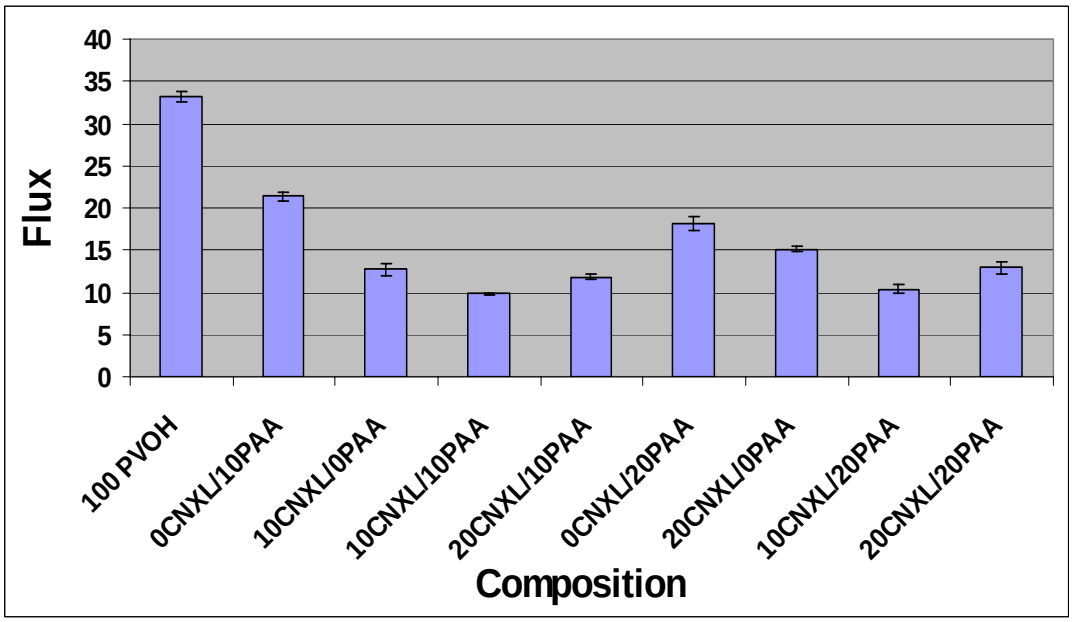

Figure 3.1. Water vapor transmission rate (WVTR) with varying weight % of PAA and CNXLs. Error bars represent one standard deviation of the means.

The optimum PAA level could be due to an optimum crosslink density for barrier properties being attained at PAA concentrations < 20%. In addition, excess of PAA may remain unreacted with the PVOH. These excess carboxyl groups should act as water absorption sites, swell the network upon contact with water[49] and as a consequence alter the flux values. However, the best barrier properties were observed with a combination of PAA and CNXLs, specifically 10% CNXLs and 10% PAA, which appeared to be a synergistic composition.

Chemical vapor transmission rate (CVTR).

The diffusion of chemical vapors through the heat treated barrier films was carried out according to ASTM standard F 1407-99a.[57] Trichloroethylene (TCE) was used as a simulant for mustard gas. Typically the TCE showed an initial unsteady flux. After a certain interval of time there was an increase in the flux, which remained constant and a steady state was then observed. The slope of this line gave the flux (g/m^2hrs). A higher lag time along with a lower flux was desired for an improved barrier film. As with the case for water, the molecules must diffuse through a tortuous path around the crystalline CNXL filler as well as through the 3D network provided by the crosslinking due to PAA. Also, PVOH by itself possesses resistance against diffusion of non polar solvents like TCE. Heat treating the pure PVOH film reduces molecular chain movement and adds crystallinity to PVOH (Fig. 2.2).

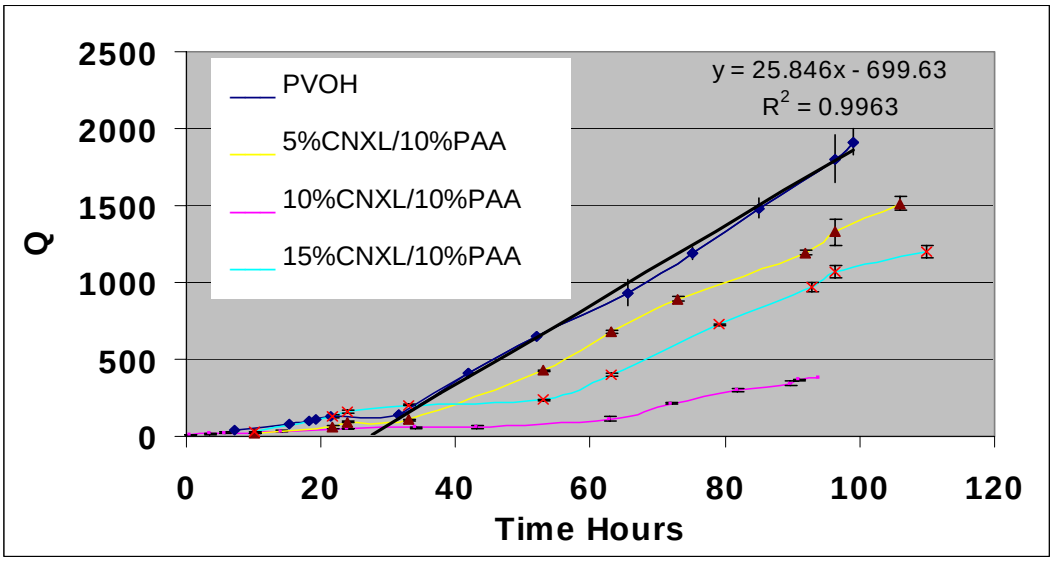

Figure 3.2. Chemical vapor transmission rate (CVTR) with varying wt % of CNXLs and 10 wt% PAA. PVOH makes up the remaining content of film. Q = Total amount of diffusion of TCE per given area at a given time (g/m^2).

For PVOH the value of 25.84 g/m^{2}hrs was obtained for the steady state flux and the time lag was 27 hours. At 5 and 10% CNXL loadings the flux was reduced and the time lag increased both without PAA and with 10% PAA (Fig. 2.2). However, at the 15% CNXL loading the flux was observed to increase and the time lag decreased compared to 10% CNXL for both 0 and 10% PAA. We attribute this to the agglomeration of CNXLs, which was observed optically (see below).

The addition of PAA had a remarkable effect on both time lag and flux (Fig. 2.2), increasing the time lag from 32 to 48 h and reducing the flux from 22 to 8 (compared to 10% CNXL, 0% PAA). Compared to 100% PVOH, the 10% PAA/10% CNXL combination increased the time lag by 90% and reduced the flux by 65%. The combination of 10% PAA/10% CNXL provided for the best barrier properties of any of the compositions tested.

Properties with carboxylated CNXLs.

In an effort to further improve the performance, the surface of the CNXLs were modified by carboxylation. The purpose of the carboxylation was to improve the bonding between the CNXLs and the PVOH. It was thought that this might reduce the need for PAA and thus improve the barrier properties and reduce the brittleness of the resulting film. The surface modification followed the method of Araki et al.[58] which results in selective oxidation of the surface C6 carbon of the anhydroglucose repeat unit of cellulose.

Carboxylation of the CNXLs was quantified by titration with 0.01 N NaOH, which indicated the presence of 1.4 mmols of acid/g CNXL. Titration of PAA with 0.5 N NaOH indicated the presence of 13.2 mmols of acid/g PAA. In the previous work it was concluded that composite film with 10% CNXLs/ 10%PAA/ 80%PVOH had the greatest interaction between the components. The amount acid groups in those films with 10%PAA was 1.32 mmols. In the composite films made with carboxylated cellulose nanocrystals (C.CNXLs) the acid groups in C.CNXLs were calculated and then PAA was added in a calculated amount so the total mmols of acid remained equal to acid content in films with 10wt % PAA (1.32 mmols of acid group). The mmols of acid groups from C.CNXLs was much lower compared to mmols of acid groups from PAA. (Figure 3.3)

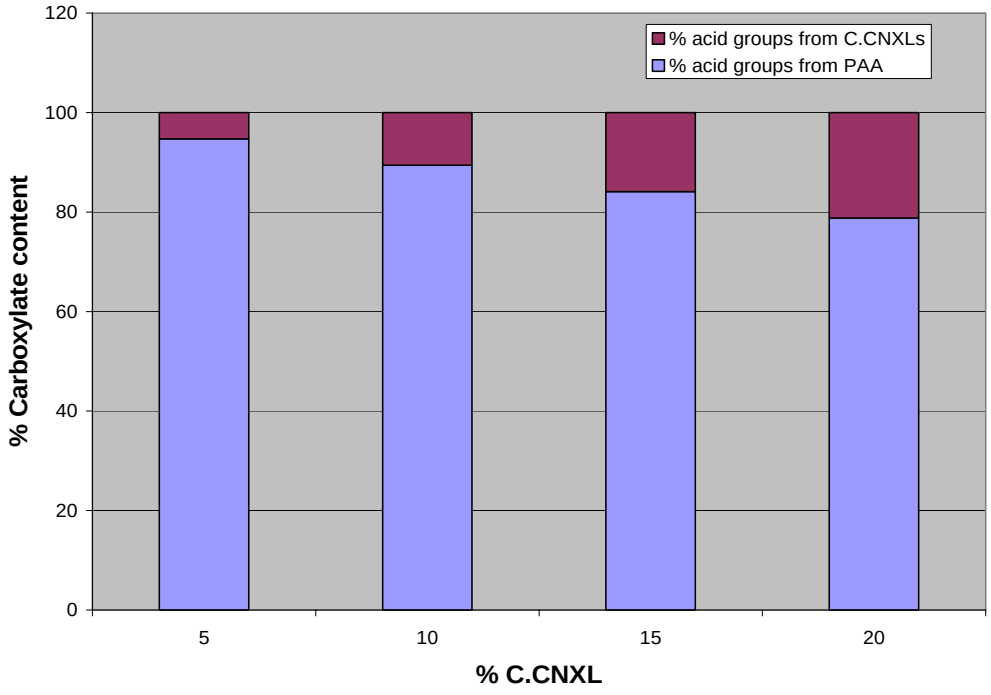

Figure 3.3. Comparison of % acid content from PAA and C.CNXLs

Fourier transform infrared spectroscopy (FTIR).

CNXLs showed a carbonyl band at 1640-1650 cm^{-1}, presumably due to some oxidation taking place during the acid hydrolysis reaction (Figure 3.4A). Carboxylation introduced an additional band at 1728 cm^{-1} (Figure 3.3B). Both the peaks are also present in a composite film with 10% carboxylated cellulose (10% C.CNXL)/ 90% PVOH (Figure 3.3C). The carboxylated content is small compared to other prominent groups like hydroxl group and hence the peak appears to be small.

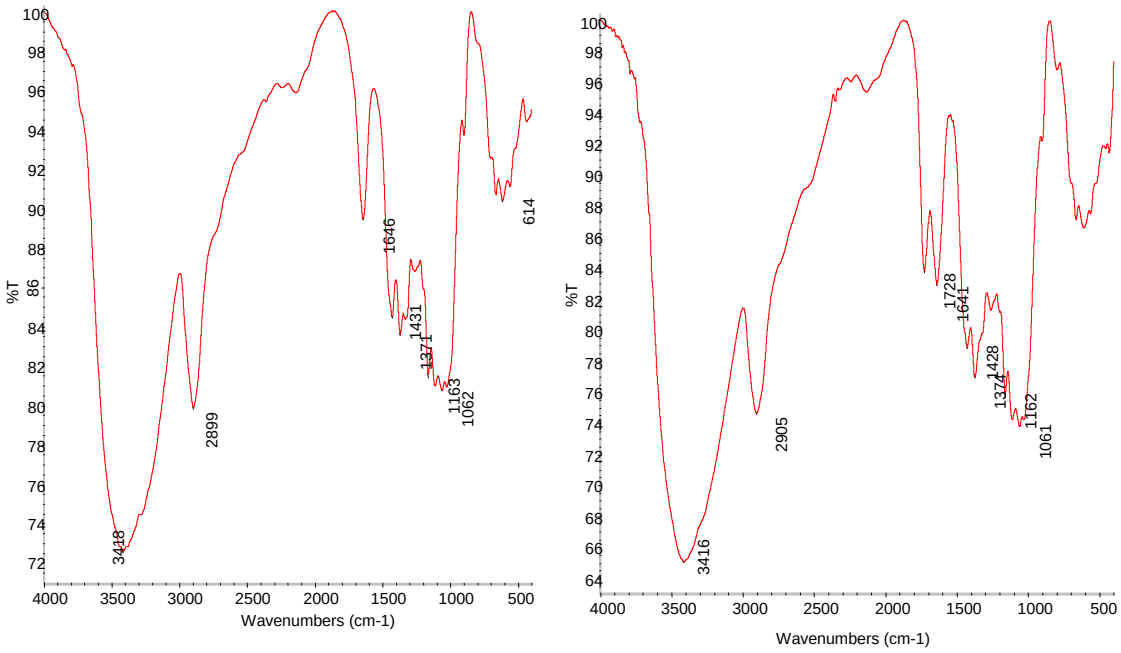

A **B**

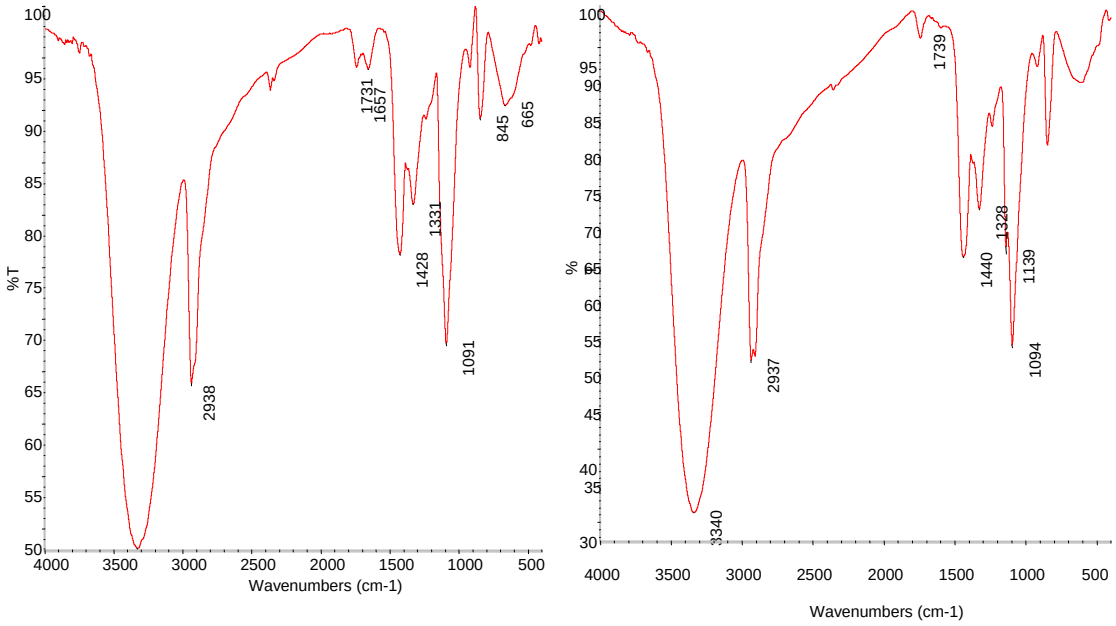

C **D**

Figure 3.4. FT-IR spectra of (A) Cellulose nanocrystals (CNXLs). (B) Carboxylated cellulose nanocrystals (C.CNXLs). (C) 10wt% C.CNXLs + 90 wt % Poly(vinyl alcohol) (PVOH). (D) Heat treated (170 °C, 45 minutes) 10wt% C.CNXLs + 90 wt % PVOH.

A heat treated composite film with 10% C.CNXL / 90% PVOH showed only one peak at 1739 cm^{-1}. The cabonyl peak at 1640-1650 cm^{-1} dissappears which could be shifting to merge with the band at 1730-1740 cm^{-1}. The band at 1730-1740 cm^{-1} could be the acid form of the carboxylic acid groups and/or could be the from the ester groups formed with heat treatment. The carbonyl peak at 1640-1650 cm^{-1} might also possibly be oxidized by the heat treatment. This would explain its absence in the spectra of heat treated samples.

Atomic force microscopy (AFM).

Atomic force microscope (AFM) of dried dispersion of nanoparticles with carboxylated cellulose (Figure 3.5B) and non carboxylated cellulose (Figure 3.5A) are compared in Figure 3.5.

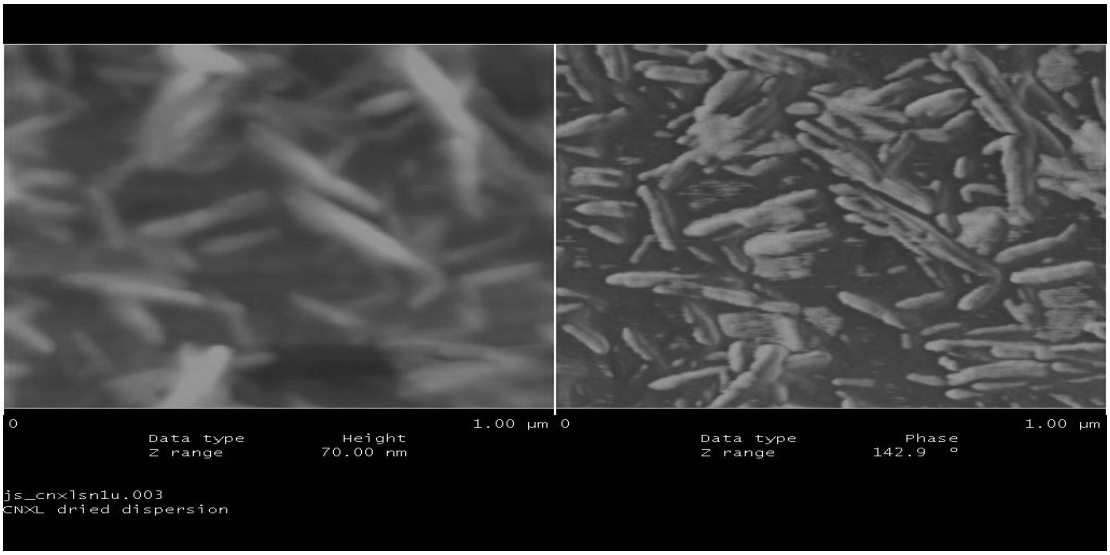

A

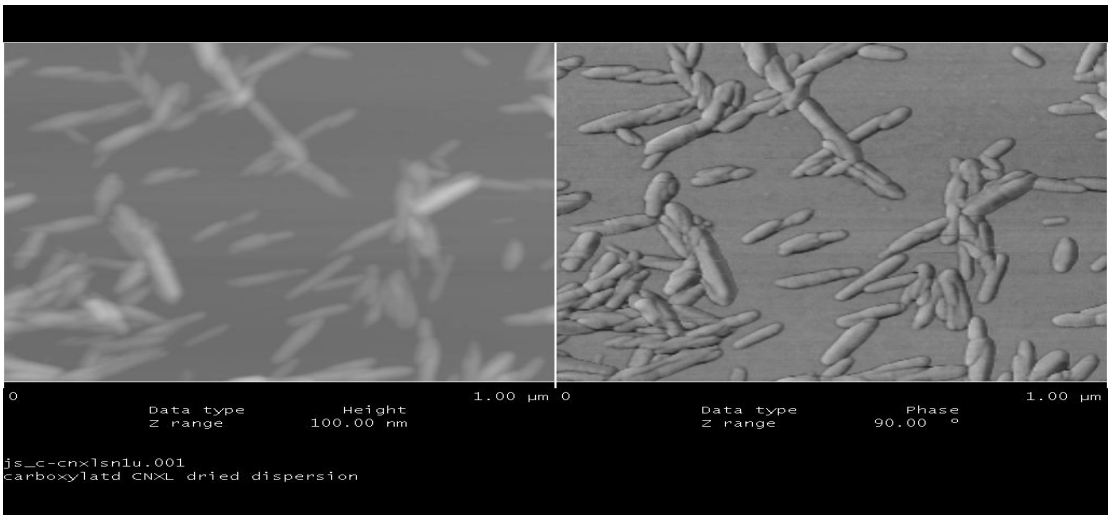

B

Figure 3.5. Atomic force microscopy (AFM) imaging in tapping mode. (A) Dried dispersion of cellulose nanocrystals (CNXLs). (B) Dried dispersion of carboxylated cellulose nanocrystals (C.CNXLs)

AFM images were observed to check if carboxylation lead to alter the length or diameter of CNXLs. Figure 3.5 indicated that carboxylation does not appear to change the physical dimensions of the individual nanocrystals.

Polarized optical microscopy.

Dispersion of C.CNXL was observed using a polarized optical microscope (Figure 3.6). At 10 wt% filler content the dispersion of CNXLs and C.CNXLs looked similar, while a pronounced difference was observed with 15 % filler content. The surface modification clearly improved the dispersion of C.CNXLs and allowed higher filler content without agglomeration.

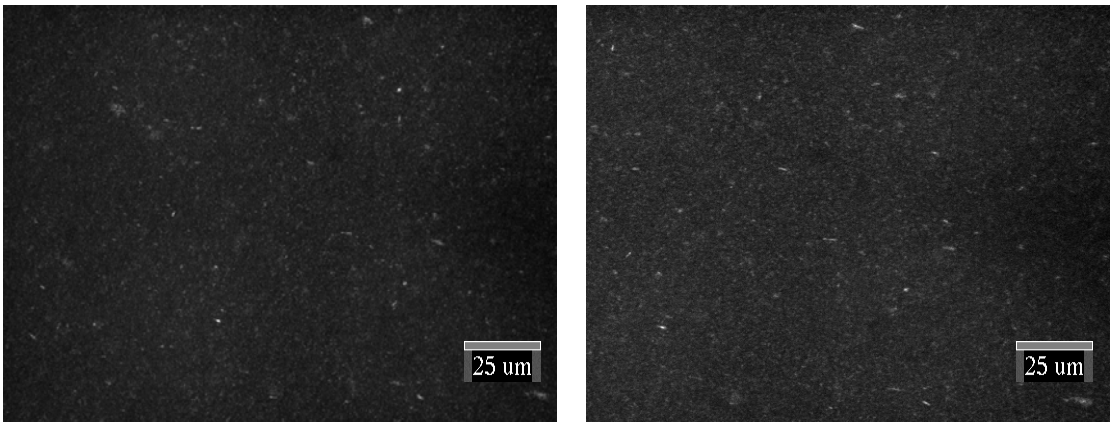

A **B**

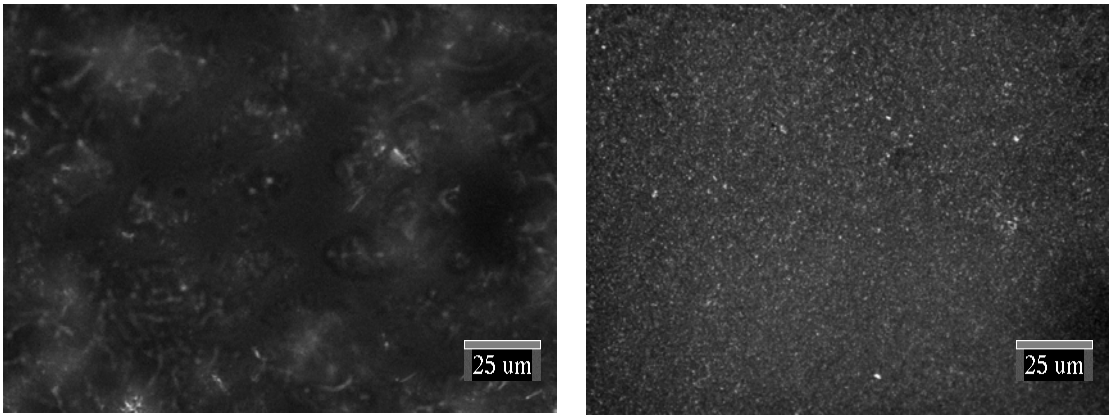

C **D**

Figure 3.6. Polarized optical microscopy pictures with (A) 10wt % CNXL/ 10wt % PAA. (B) 10wt % C.CNXL/ 10wt % PAA. (C) 15wt% CNXL/ 10wt% PAA. (D) 15wt% C.CNXL/ 10wt% PAA. PVOH makes up the remaining content of the films.

Scanning electron microscopy (SEM).

SEM images of fractured surfaces showed a rough fracture for heat treated 10 %CNXL/10%PAA/ 80%PVOH film (Fig. 3.7A). Crack initiation was observed but good bonding prevented further crack propagation. The heat treated film with 10 % C.CNXL/ PAA/ PVOH showed a smooth flaky fractured surface (Fig. 3.7B). Evidently, the interaction between the components improved in the presence of C.CNXLs.

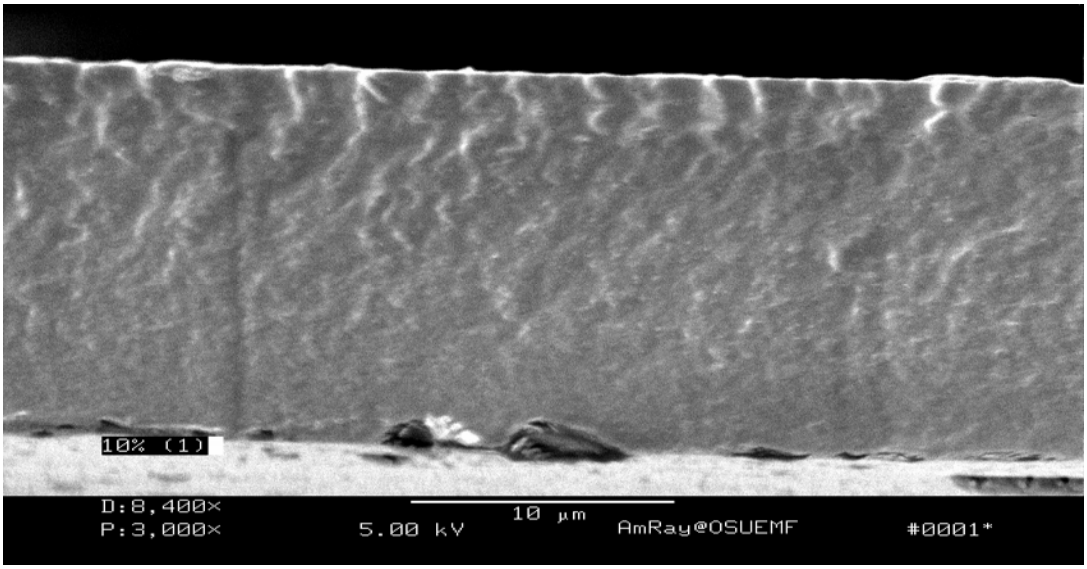

A

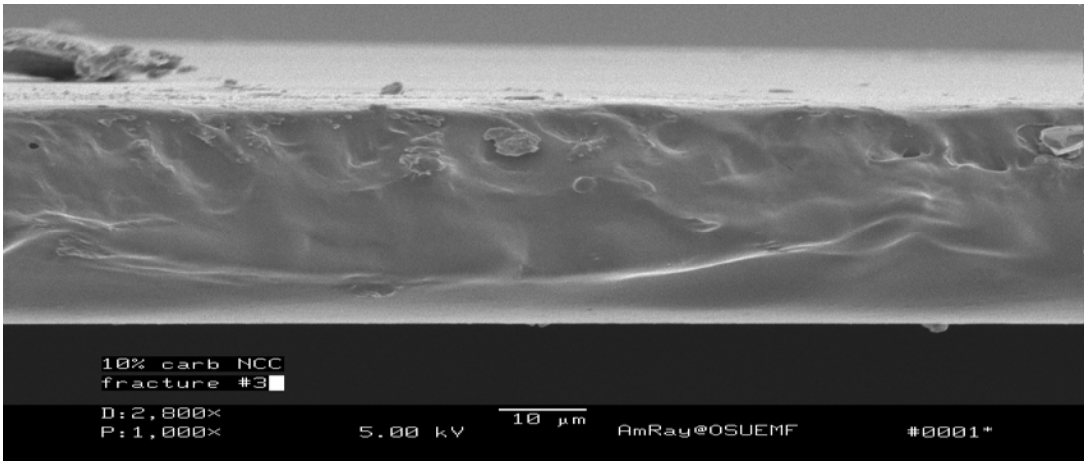

B

Figure 3.7. Fractured surface images by SEM. (A) 10% CNXLs/ 10 % PAA/ 80% PVOH (B) 10% C.CNXLs/10 % PAA/ 80 % PVOH. Films were heat treated at 170 °C for 45 minutes before fracturing.

Water vapor transmission rate.

WVTR with C.CNXLs showed slight improvement compared to non carboxylated CNXLs at all levels, both with and without PAA (Fig. 3.8). Increases in WVTR were observed for the 20% CNXL loading for both carboxylated and non-

carboxylated. This is perhaps due to increased agglomeration at this high loading.

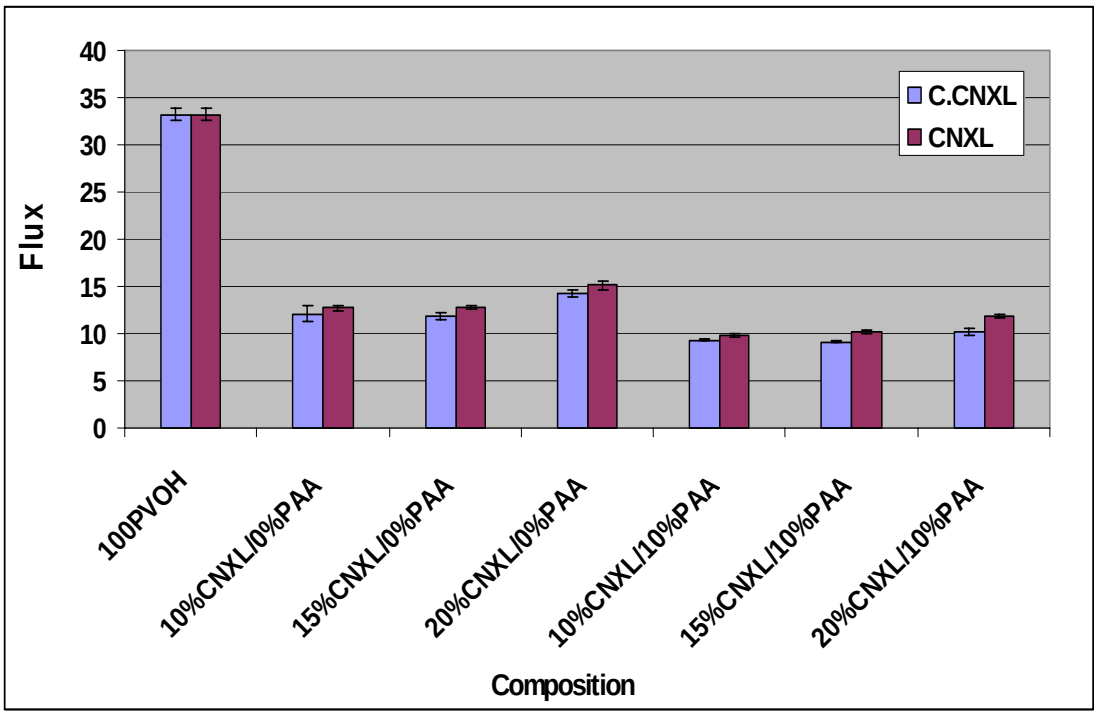

Figure 3.8. Water vapor transmission rate (WVTR) with varying weight % of cellulose nanocrystals (CNXLs/C.CNXLs) and varying weight % of PAA. Acid content (mmols) of C.CNXL+PAA = Acid content (mmols) of 10wt% PAA. PVOH makes up the remaining content of the films.

Chemical vapor transmission rate (CVTR).

Combined with the optical microscopy results, these data suggest that the 15% C.CNXL is better dispersed than the non-carboxylated version. However, agglomeration is probably having an effect at the 20% loading even in the C.CNXL case. Chemical vapor transmission rate with C.CNXLs and CNXLs with no PAA when compared (Figure 3.9A) indicated lower flux and minor increase in time lag.

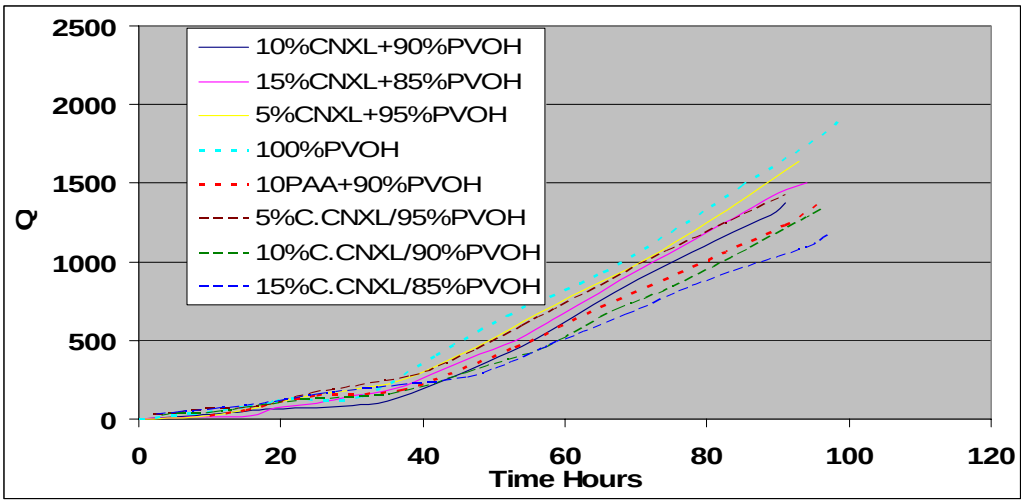

A

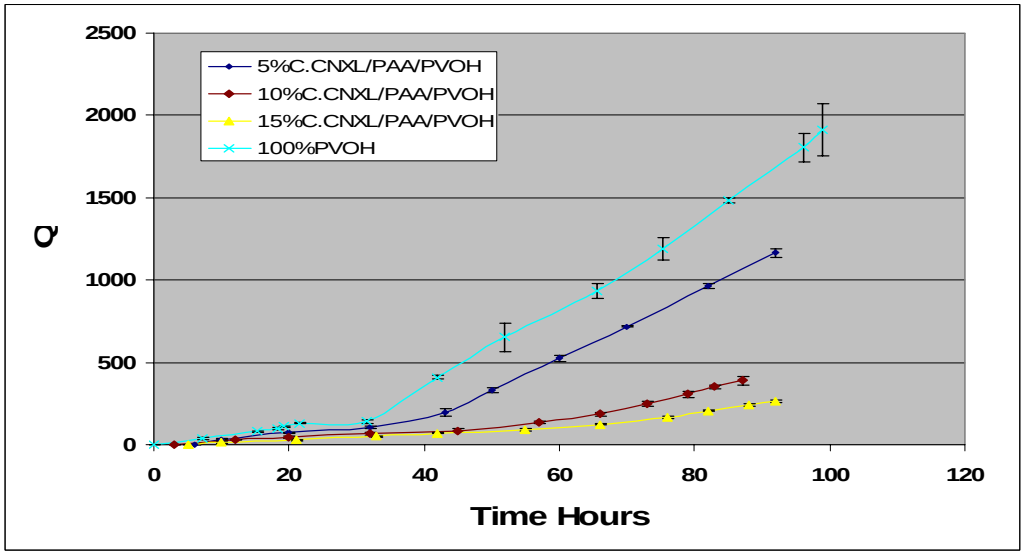

B

Figure 3.9. Chemical vapor transmission rate (CVTR) (A) Comparing films with varying amounts of CNXLs with C.CNXLs. (B) Films with varying content of C.CNXL. Acid content (mmols) of C.CNXL+PAA = Acid content (mmols) of 10wt% PAA. PVOH makes up the remaining content of the films. Q = Total amount of diffusion of TCE per given area at a given time (g/m^2).

In the presence of PAA, but with the amount of PAA reduced to keep the amount of carboxylic groups present in the sample constant (Figure 3.10 or Appendix

Table B.2), we again observed improved performance due to carboxylation of the CNXLs, but the improvement was usually quite small or nonexistent in the case of flux in the 10% PAA/10% CNXL (Fig. 3.10D). The exception is the large reduction in flux for both carboxylated and non-carboxylated and large decrease in flux for carboxylated CNXLs at the 15% CNXL addition level. We speculate this is due to the agglomeration of CNXLs and the lack of agglomeration in the C.CNXLs at the 15% level.

It appears that improving covalent bond formation between the CNXLs and the matrix did not offer much improvement in performance. The presence of PAA, especially at the 10% addition level, had a much stronger influence in CVTR than carboxylation of the CNXLs. Apparently the total crosslink density is more important than controlling the interface chemistry in terms of CVTR performance.

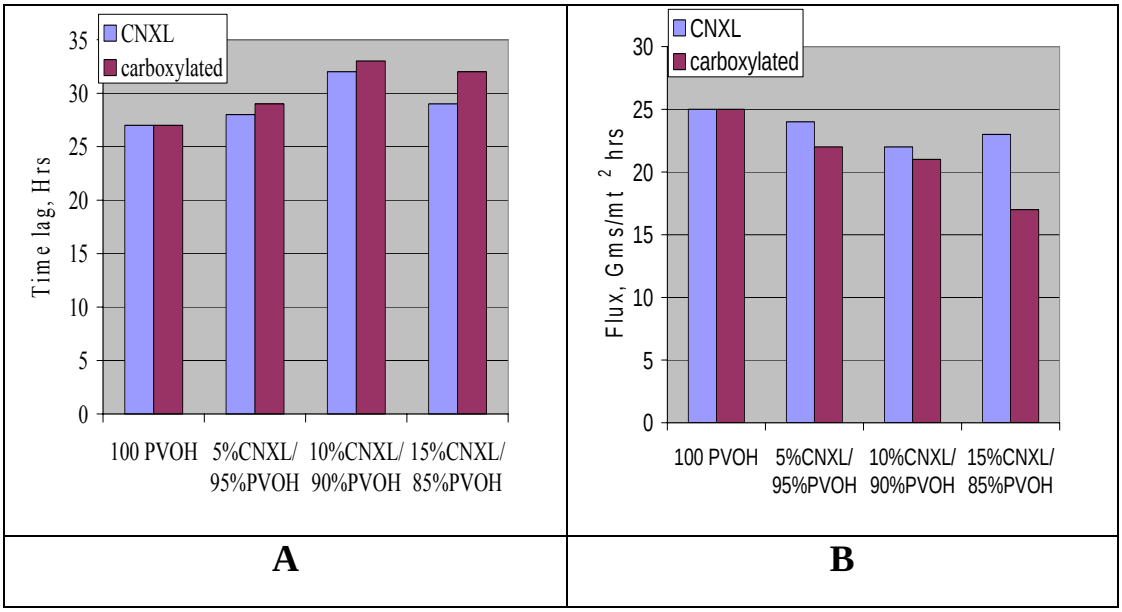

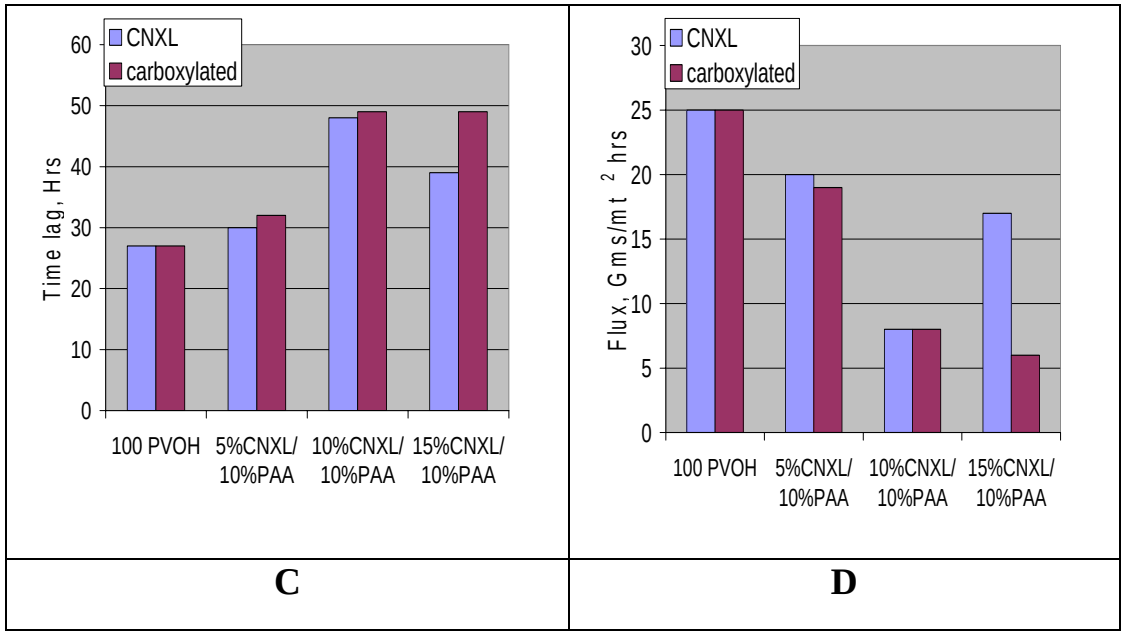

Figure 3.10. Summary of results from Chemical vapor transmission rate (CVTR) comparing carboxylated (C.CNXLs) and non carboxylated cellulose nanocrystals (CNXLs). (A) Time lag (Hours) for the films with no Poly(acrylic acid) (PAA). (B) Flux (g/m^2 hr) for the films with no Poly(acrylic acid) (PAA). (C) Time lag (Hours) for films with Poly(acrylic acid) (PAA). (D) Flux (g/m^2 hr) for films with Poly(acrylic acid) (PAA).

Mechanical testing.

Filled nanocomposites have been shown to improve both tensile modulus and elasticity.[33, 34] Mechanical test indicated use of C.CNXLs resulted in a slight embrittlement of the nanocomposite, with the % elongation reduced. Carboxylation also gave a slight increase in modulus compared to non-carboxylated version. UTS and energy to break were equivalent for both carboxylated and non-carboxylated. (Fig. 3.11).

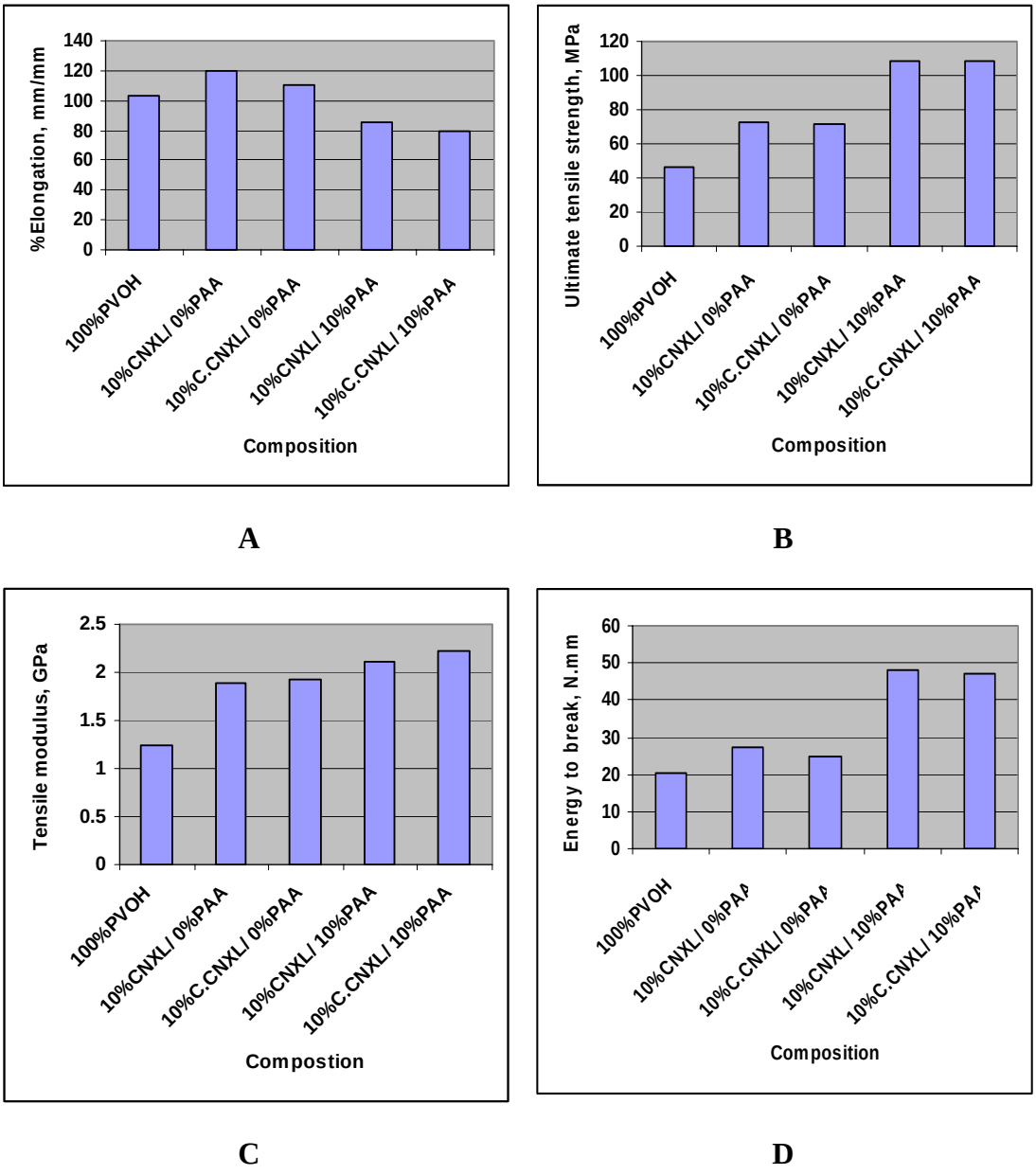

Figure 3.11. Sintech tensile test charts (A) % Elongation. (B) Ultimate tensile strength. (C) Tensile modulus. (D) Energy to break (Toughness).

These results are consistent with our hypothesis that carboxylating the CNXLs increased ester bond formation between the CNXLs and the polymer matrix.

Thermal gravimetric analysis.

Previous work (Chapter 2) showed that the combination of CNXLs, PVOH and PAA raised the initial degradation temperature dramatically from those of the individual components. We interpret this to mean that there are strong associations, indeed crosslinking ester bonds, between the various components. TGA scans of C.CNXLs supports this contention as the degradation temperature of the composite is raised an additional 40 °C as compared to non C.CNXLs (Figure 3.12). This large shift indicates even greater interaction between the components due to surface modification of the CNXLs. This ~100 °C increase in degradation temperature may allow for increased applications of this material, or may reduce the need for fire retardants to be added to the final commercial formulation.

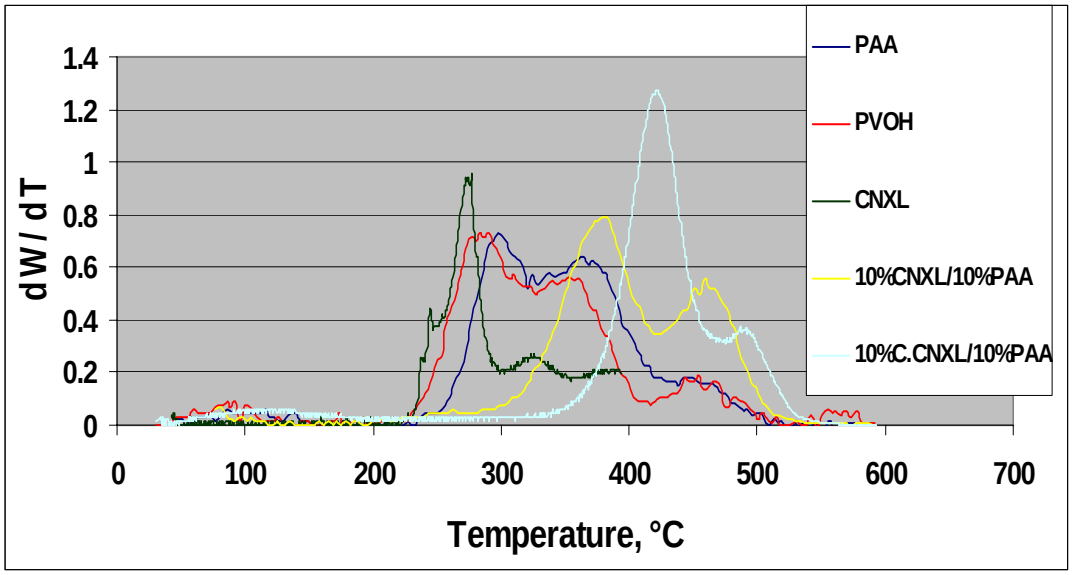

Figure 3.12. DTGA graphs showing the thermal degradation of pure components and films with 10% PAA/ 10% CNXLs/C.CNXLs.

Conclusions

Previous work (Chapter 2) suggested heat treated film with 10%CNXL/ 10%PAA/ 80%PVOH showed highly synergistic effects and improved mechanical properties. The CVTR experiments show 90% increase in the lag time and the flux reduced by 65% compared to pure PVOH film. Though, the data do not allow a firm conclusion that CNXLs are chemically bonded with the film matrix, certainly their presence alters the lag time as well as the flux of both water and TCE and hence improves the barrier properties. All the films allowed moisture to pass through at a reasonable rate. Surface modification of cellulose nanocrystals was successful in grafting carboxylic acid groups, presumably to the C_6 carbon. Various microscopies showed better dispersion with C.CNXLs and suggested filler contents up to 15 wt% could be tolerated without agglomeration. CVTR experiments showed C.CNXLs slightly reduced flux and increased time lag compared to CNXLs as a result of better confirmation with the matrix. C.CNXLs increased stiffness and reduced % elongation; hence the overall energy to break (toughness) does not alter to a great extent. The differential thermal gravimetric analysis (DTGA) showed a large increase of 40 °C in the temperature of maximum rate of degradation which suggested C.CNXLs had greater interaction within the matrix, presumably ester bond formation.

Acknowledgement

We gratefully acknowledge the support from the National Research Initiative of the USDA Cooperative State Research, Education and Extension Service, grant number 2003-35103-13711.

Thesis conclusions

Conclusions

Heat treatment improved the crosslinking density within the films made of varying contents of CNXL, PAA and PVOH. Solubility results indicate that higher temperature heat treatments result in higher crosslink density within the matrix. The optimum heat treatment suggested from this work is 170 °C for 45 min. The FTIR spectrum indicates heat treatment results in formation of ester linkages between PAA and PVOH. CNXLs were well dispersed in blended films of PVOH and PAA at 10 % content by weight, but agglomerated at 20%. This result is supported by AFM and optical microscopy images. The presence of CNXLs and crosslinking almost doubles the strength, stiffness and toughness, while the elongation is reduced by 20%. The DTGA suggests close association between PVOH and CNXL without the presence of PAA. The DTGA results show a synergistic effect of 10% CNXLs and 10% PAA in a PVOH matrix. Overall, the heat treated film with 10%CNXL/ 10%PAA/ 80%PVOH had well-dispersed cellulose nanocrystals and effective interactions between the components which resulted in improved mechanical properties. This combination holds promise and was tested further for its barrier properties.

All the films tested for water vapor transmission with varying composition of CNXL, PAA and PVOH allowed moisture to pass through reasonably well. Barrier films require moisture to pass through so breathable clothing can be manufactured. The CVTR experiments showed a 90% increase in the lag time and the flux reduced by 65% for 10%CNXL/ 10%PAA/ 80%PVOH, compared to pure PVOH film.

Though, it cannot be said if CNXLs are chemically bonded with the film matrix, their presence alters the lag time as well as the flux of chemicals and hence improves the barrier to diffusion of toxic chemicals. Surface modification of cellulose nanocrystals was successful in adding carboxylic acid groups, presumably to the C_6 carbon. Various microscopies showed better dispersion with C.CNXLs compared to CNXLs and allowed higher filler contents in the films up to 15 wt%. CVTR experiments showed C.CNXLs reduced flux and increased time lag compared to CNXLs, presumably as a result of improved bonding with the matrix. C.CNXLs increased stiffness and reduced % elongation; hence the overall energy to break (toughness) does not alter to a great extent. The differential thermal gravimetric analysis (DTGA) showed a large shift of 40 °C which suggested C.CNXLs had stronger interactions, probably ester formation, with the matrix.

Suggestions for future work

The film prepared and tested in this project is only a part of the composite product which will be used for protection shelters. The film will be sprayed or applied over a cloth material and will be covered with a third material which will be water proof. Further testing will be required with the whole assembly. The longetivity of the material, packing volume, overall cost and ease of sealing together have to be tested before commercial utility can be determined. The films tested in this project are 25-27 microns, while the actual films might be around 50 microns thick. The thermal, mechanical and diffusivity properties of the films may vary with thickness of the films as the dispersion of CNXLs within these films might be different. The chemical vapor

transmission rate greatly depends upon the dispersion of CNXLs within the film. So, it is essential to test the dispersion of CNXLs and the changes created thereby with films of the final commercial thickness. Humidity and temperature also play an important role in the rate of diffusion through a polymeric film. These tests should be repeated with the films in various humidity and temperature chambers to analyse those effects on the final properties.

Appendix

A.1 Procedure to prepare of PVOH / PAA solutions.

1. For 100 mls of the final solution (5 wt%), take 5 gms of the powder form. 2. Take 95 gms of DI water in a beaker. 3. Set the oil bath at 85 °C temperature. 4. Put the water beaker in the oil bath and set the stirrer at a medium speed. 5. Once the temperature reaches around 50 °C, start adding PVOH / PAA powder grain by grain. 6. After the previously added powder is completely wet by the water add some more powder. 7. Maintain the temperature at 85 °C for ½ hour to obtain a clear solution. 8. Measure the contents in a measuring cylinder and add make up DI water, if some has evaporated during heating.

A.2 Procedure to prepare cellulose nanocrystals.

1. Grind Whatman #1 filter paper to a fine powder which can pass through a 40 mesh screen. 2. Partially hydrolyse ground paper with 65 % H_2SO_4 (v/v) solution at 45 °C with medium stirring for 50 minutes. The ground paper to acid ratio was 1:10 g/mL. 3. Centrifuge the resulting mixture 5 times with DI water to remove the spent acid. 4. Subject the suspension to ultrasonic irradiation in the branson sonifier for 15 minutes to disperse the CNXLs and break any agglomerates formed. 5. Disintegrate the supension further in the warring blender for 15 minutes. 6. Ultrafiltered the suspension to remove microparticulates and ions until the conductivity was <10

μS/cm. 7. Concentrated the dispersion in a rotavaporizer R110 to obtain an aqueous dispersion of 1% CNXLs. 8. Test the % solids.

A.3 Procedure to prepare films.

(Example of 10% CNXL/ 10% PAA/ 80% PVOH is provided)

1. Stir all solutions (5% PVOH, 5% PAA, 1% CNXLs) to avoid settling or concentration difference. 2. Take 16 mls PVOH/ 2 mls PAA/ 10mls CNXLs to prepare a blend solution with the desired % solids. 3. Sonicate the blend for 20 minutes. 4. Arrange 8 cm diameter plastic dish on a flat surface with the use of water balance. Use thin paper or glass cover slides to obtain even thickness. 5. Pour 5 mls of blend solution over the dish and allow to air dry for around 40 hours. 6. Heat treat the formed films, after putting them in an aluminium pan, in upper compartment of the convection oven at 170 °C for 45 minutes.

A.4 Procedure to prepare carboxylated cellulose.

1. Take 200 mL of 1% cellulose nanocrystal dispersion in a round bottom flask, then add 0.2 gm of TEMPO and 2 gm of NaBr. 2. Initiate the oxidation reaction by adding 10mL of NaClO solution. Allow constant stirring at slow speed. Attach a burette with 1 N NaOH solution with a pH meter and maintain a constant pH of 10. 3. Subsequently, add 10 mL NaClO after 2 and 4 hours. The overall reaction time is 15 hours and a pH of 10 is maintained throughout. 4. Discontinue the oxidation reaction with the addition of 30 mL of ethanol. 5. Ultrafilter the suspension thrice to remove

unreacted reagents. 6. Add 2 mls of pure HCl to convert the carboxyls to free acid. 7. Ultrafiltered the solution again until a conductivity of < 5 μS/cm is obtained. 8. Concentrate the dispersion in rotavaporizer R110 to obtain 1 % carboxylated CNXLs dispersion. 9. Calculate the carboxylated content (mmols of acid group) of the dispersion by titrating against 0.01 N NaOH.

Appendix Tables

Table B.1. Density and cost comparison between some of the frequently used reinforcing fillers.

Materials	Density (g/cm^3)	Cost($/kg)
Glass Fibers	**2.6**	**1.30-2.00**
Flax	**1.5**	**0.22-1.1**
Cellulose	**1.5**	**1.8-2.0**
Aramid	**1.45**	**22-33**
Boron	**2.45**	**330-440**

Table B.2. Results from chemical vapor transmission rate experiments.

Film composition	Time Lag (Hours)	Flux (G/m^2hrs)
100PVOH	**27**	**25**
10%PAA / 90%PVOH	**29**	**20**
5%CNXL/ 95%PVOH	**28**	**24**
10%CNXL/ 90%PVOH	**32**	**22**
15%CNXL/ 85%PVOH	**29**	**23**
5%C.CNXL/ 95%PVOH	**29**	**22**
10%C.CNXL/ 90%PVOH	**33**	**21**
15%C.CNXL/ 85%PVOH	**32**	**17**
5%CNXL/ 10%PAA	**30**	**20**
10%CNXL/ 10%PAA	**48**	**8**
15%CNXL/ 10%PAA	**39**	**17**
5%C.CNXL/ 10%PAA	**32**	**19**
10%C.CNXL/ 10%PAA	**49**	**8**
15%C.CNXL/ 10%PAA	**49**	**6**

Bibliography

1. Havancsak K., Nanotechnology at present and its promises in the future. *Material Science Forum* **2003,** 414-415, 85-94.

2. NASA., http://www.ipt.arc.nasa.gov/nanotechnology.html.

3. Bor J., Advanced polymer composites; ASM International: Materials Park, **1994**, 1-279.

4. Brechet Y; Cavaille J; Chabert E; Chazeau L; Dendievel R; Flandin L; Gauthier C., Polymer based nanocomposites: Effect of filler-filler and filler-matrix interactions. *Advanced engineering materials* **2001,** 3, 571.207.

5. Giannelis E., Polymer-Layered silicate nanocomposites: Synthesis, properties and applications. *Applied organometallic chemistry* **1998,** 12, 675-680.

6. Favier V; J, C., Polymer Nanocomposites reinforced by cellulose whiskers. *Macromolecules* **1995,** 28, (18), 6365-6367.

7. Dufresne A; Kellerhals M; Witholt B., Transcrystallization in Mcl-PHAs/Cellulose whiskers composites. *Macromolecules* **1999,** 32, 7396.

8. Eichhorn S; Baillie C; Zafereiropoulos N; Mwaikambo L; Ansell M; Dufresne A; Entwistle K; Herrera-Franco P; Escamilla G; Groom L; Hughes M; Hill C; Rials T., Review- Current international research into cellulosic fibres and composites. *Journal of Material Science* **2001,** 36, 2107.

9. Marks R., Cell wall mechanics of tracheids. *Cell wall mechanics of tracheids;* Yale University press: New Haven, **1967**.

10. Hon D., Chemical modification of lignocellulosic materials; Marcel Dekker Inc.: New York, **1996**, 36.

11. Ranby G., The colloidal properties of cellulose micelles. *Discussions Faraday Society* **1951,** 11, 158-164.

12. Millet M; Moore W; Saeman J., Preparation and properties of hydrocelluloses. *Industrial Engineering Journal* **1954,** 46, 1493-1497.

13. Dong X; Revol J; Gray D., Effect of microcrystallite preparation conditions on the formation of colloid crystals of cellulose. *Cellulose* **1998,** 5, (1), 19-32.

14. Crank J; Park G., Diffusion in polymers; Academic Press: New York, **1968**, 1-40.

15. Finch C., Polyvinyl alcohol developments; John Wiley & Sons: New York, **1992**.

16. Arndt K; Richter A; Ludwig S; Zimmermann J; Kressker J; Kuckling D; Alder H., Poly(vinyl alcohol)/ poly(acrylic acid) hydrogels: FT-IR spectroscopic characterization of crosslinking reaction and work at transition point. *Acta Polymers* **1999,** 50, 383-390.

17. Kumeta K; Nagashima I; Matsui S; Mizoguchi K., Crosslinking reaction of poly(vinyl alcohol) with poly(acrylic acid) by heat treatment: Effect of neutralization of PAA. *Journal of Applied Polymer Science* **2003,** 90, 2420-2427.

18. Sanli O; AsmanG., Release of diclofenac through gluteraldehyde crosslinked poly(vinyl alcohol) / poly(acrylic acid) alloy membranes. *Journal of Applied Polymer Science* **2003,** 91.

19. Donahue K., Chemical and biological barrier materials for collective protection shelters. *http://nsc.natick.army.mil/jocotas/ColPro_Papers/Donahue.pdf* **2004**.

20. Krishnamoorti R; Vaia A., Polymer Nanocomposites: Synthesis, characterization and modeling. *ACS Symposium Series* **2001**.

21. Brechet Y; Cavaille J; Chabert E; Chazeau L; Dendievel R; Flandin L; Gauthier C., Polymer based nanocomposites: Effect of filler-filler and filler-matrix interactions. *Advanced engineering materials.* **2001,** 3, (8), 571-207.

22. Gacitua W; Ballerini A; Zang J., Polymer nanocomposites: synthetic and natural fillers- A review. *Maderas. Ciencia y technologia* **2005,** 7, (3), 159-178.

23. Cao G., Nanostructures & Nanomaterials: Synthesis, properties & Applications. **2004**.

24. Fakhouri F; Tanada-Palmu P; Grosso C., Characterization of composite biofilms of wheat gluten and cellulose acetate phthalate. *Brazilian Journal of Chemical Engineering.* **2004,** 21, 261-264.

25. Flaconneche B; Martin J; Klopffer M, Transport properties of Gases in polymers: Experimental Methods. Oil & Gas Science and Technology. *Oil & Gas Science and Technology* **2001,** 56, (3), 245-259.

26. Lu C; Mai Y., Influence of aspect ratio on barrier properties of Polymer-clay nanocomposites. *Physical Review letters* **2005,** 8, 0883031-0883034.

27. Tortora M; Vittoria V; Galli G; Ritrovati S; Chiellini E., Transport properties of modified montmorillonite-poly(e-caprolactone) nanocomposites. *Macromolecular materials and engineering* **2002,** 287, 243-249.

28. Yano K; Usuki A; Okada A., Synthesis and properties of polyimide-clay hybrid films. *Journal of Polymer Science, Part A: Polymer Chemistry* **2000,** 35, (11), 2289-2294.

29. Hasegawa N; Okamoto H; Kato M; Usuki A., Preparation and mechanical properties of polypropylene-clay hybrids based on modified polypropylene and organophilic clay. *Journal of Applied polymer science* **2000,** 78, (11), 1918-1922.

30. Ke Y; Long C; Qi Z., Crystallization, properties and crystal nanoscale morphology of PET-clay nanocomposites. *Journal of Applied polymer science* **1999,** 71, (7), 1139-1146.

31. Wang D; Parlow D; Yao Q; Wilkie C., PVC-clay nanocomposites: Preparation, thermal and mechanical properties. *Journal of Vinyl and Additive Technology* **2004,** 7, (4), 203-213.

32. Donahue K., Chemical and biological barrier materials for collective protection shelters. *http://nsc.natick.army.mil/jocotas/ColPro_Papers/Donahue.pdf*, **2004**.

33. Orts J; Shey J; Imann S; Glenn G; Guttman M; Revol J., Application of cellulose microfibrils in polymer nanocomposites. *Journal of polymers and the environment.* **2005,** 13, (4), 301-306.

34. Bledzki A; Gassan J., Composites reinforced with cellulose based fibers. *Progress in polymer science.* **1999,** 24, 221-274.

35. Zimmermann, T; Pohler E; Geiger T., Cellulose fibrils for polymer reinforcement. *Advanced engineering materials* **2004,** 6, (9), 754-761.

36. Sturcova A; Davies G; Eichhorn S., Elastic modulus and stress transfer properties of tunicate cellulose whiskers. *Biomacromolecules* **2005,** 6, 1055-1061.

37. Fabiola V; Paijs T., Cellulose based nanocomposites. *Forest Products Society* **2005**, 283-295.

38. Marks R., Cell wall mechanics of tracheids. *Cell wall mechanics of tracheid*; Yale University press: New Haven,, **1967**.

39. Borges J; Godinho M; Belgacem M; Martins F., New bio-composites based on short fibre reinforced hydroxypropylcellulose films. *Composite interfaces* **2001,** 8, (3), 233-241.

40. Finch C., Polyvinyl alcohol developments; John Wiley & Sons: New York, **1992**.

41. Bourke S; Al-Khalili M; Briggs T; Michniak B; Kohn J; Poole-Warren L., A Photo-crosslinked Poly(vinyl alcohol) hrdrogel growth factor release vehicle for wound healing applications. *AAPS PharmaSci* **2003,** 5, (4), 33.

42. Lange J; Wyser Y., Recent innovations in barrier technologies for plastic packaging - a review. *Packaging Technology and Science* **2003,** 16, (4), 149-158.

43. Wan W; Campbell G; Zhang Z; Hui A; Boughner D., Optimizing the tensile properties of poly(vinyl alcohol) hydrogel for the construction of a bioprosthetic heart valve stent. *Journal of Biomedical Materials Research* **2002,** 63, (6), 854-861.

44. Schmedlen R; Masters K; West J., Photocrosslinkable polyvinyl alcohol hydrogels that can be modified with cell adhesion peptides for the use in tissue engineering. *Biomaterials* **2002,** 23, (22), 4325-4332.

45. Kumeta K; Nagashima I; Matsui S; Mizoguchi K., Crosslinking reaction of poly(vinyl alcohol) with poly(acrylic acid) by heat treatment: Effect of neutralization of PAA. *Journal of Applied polymer science* **2003,** 90, 2420-2427.

46. Arndt K; Richter A; Ludwig S; Zimmermann J; Kressker J; Kuckling D; Alder H., Poly(vinyl alcohol)/ poly(acrylic acid) hydrogels: FT-IR spectroscopic characterization of crosslinking reaction and work at transition point. *Acta polymers* **1999,** 50, 383-390.

47. Hassan C; Peppas N., Structure and applications of poly(vinyl alcohol) hydrogels produced by conventional crosslinking or by freezing/thawing methods. *Advances in Polymer Science* **2000,** 153, 37-65.

48. McCrum N; Read B; Williams G., Anelastic and Dielectric Effects in Polymeric Solids. *Wiley* **1967**.

49. Sanli O; Asman G., Release of diclofenac through gluteraldehyde crosslinked poly(vinyl alcohol)/ poly(acrylic acid) alloy membranes. *Journal of Applied polymer science* **2003,** 91, 72-77.

50. Asman G; Sanli O., Characteristics of permeation and separation for acetic acid-water mixtures through poly(vinyl alcohol) membranes modified with poly(acrylic acid). *Separation science and technology* **2003,** 38, 1963-1980.

51. Peppas N; Wright S., Solute Diffusion in poly(vinyl alcohol)/poly(acrylic acid) interpenetrating networks. *Macromolecules* **1996,** 29, 8798-8804.

52. Rhim J; Kim H; Lee K., Pervaporation separation of binary organic-aqueous liquid mixtures using crosslinked poly(vinyl alcohol) membranes IV. Methanol-Water mixture. *Journal of Applied Polymer science.* **1996,** 61, 1767-1771.

53. Choi Y., Cellulose nanocrystals filled carboxymethyl cellulose composites. *Thesis* **2005**.

54. Flaconneche B; Martin J; Klopffer M., Transport properties of Gases in polymers: Experimental Methods. Oil & Gas Science and Technology. *Oil & Gas Science and Technology* **2001,** 56, (3), 245-259.

55. Hannoun B; Stephanopoulos G., Diffusion coefficients of glucose and ethanol in cell free and cell occupied calcium alginate membranes. *Biotechnology and Bioengineering* **1986,** 28, (6), 829-835.

56. Crank J; Park G., Diffusion in Polymers; *Academic Press: London.* **1968**, 1-40.

57. Standard method of resistance of chemical protective clothing materials to liquid permeation. Permeation Cup method (Method F 1407-99a). *ASTM* **1999**.

58. Araki J; Masahisa W; Kuga S., Steric stabilization of a cellulose microcrystal suspension by oly(ethylene glycol) grafting. *Langmuir* **2001,** 17, 21-27.